

# Zn-Pb mineralization associated with a mafic dyke at Cheverie, Hants County, Nova Scotia: implications for Carboniferous metallogeny

Daniel J. Kontak<sup>1</sup>, Kevin Ansdell<sup>2</sup>, and Douglas A. Archibald<sup>3</sup>

<sup>1</sup> *Department of Natural Resources, P.O. Box 698, Halifax, Nova Scotia B3J 2T9, Canada*

<sup>2</sup> *Department of Geological Sciences, 114 Science Place, Saskatoon, Saskatchewan S7N 5E2, Canada*

<sup>3</sup> *Department of Geological Sciences, Queen's University, Kingston, Ontario K7L 3N6, Canada*

*Date Received: June 12, 2000*

*Date Accepted: August 13, 2000*

The Cheverie Zn-Pb occurrence, within the Windsor Basin of southern Nova Scotia, is associated with intense carbonate alteration of a mafic dyke and surrounding deformed dark grey siltstone and shale of the Carboniferous Horton Bluff Formation. The mafic dyke, consisting of euhedral plagioclase (An<sub>45-60</sub>), augitic pyroxene, and ilmenite with late-stage mesostasis and granophyre, is subalkaline, has within-plate affinities and is similar to E-MORB; clinopyroxene chemistry indicates a transitional subalkaline-alkaline chemistry. Dating (<sup>40</sup>Ar/<sup>39</sup>Ar whole rock) of the mafic dyke indicates emplacement at 315 Ma, thus providing a minimum age for ductile deformation of the sedimentary rocks and a maximum age for the mineralization.

The occurrence of pyrite, marcasite, sphalerite (Fe-poor and Fe-rich), and galena with bitumen is similar to the metal association at the nearby Walton barite-base metal deposit and suggests a metallogenic affinity. Two phase (L<sub>H<sub>2</sub>O</sub>-V) fluid inclusions in vein carbonate homogenize at 156° to 265°C and have salinities of 0–22 wt. % equiv. NaCl. Stable isotopes analyses indicate: (1) δ<sup>34</sup>S values of –4.5 and +2.2 ‰ for galena and –4.4 ‰ for sphalerite; and (2) δ<sup>13</sup>C values of –8.8 and –1.4 ‰ and δ<sup>18</sup>O values of +22.5 and +21.2 ‰ for carbonate, with the latter equating to +11.7 to +13.0 ‰ for formation temperatures of ca. 200°C.

The fluid chemistry is consistent with basinal-type fluids originating within the Windsor Basin and interacting with liquid petroleum and other lower-temperature and lower-salinity fluids. A similar fluid history has been inferred for the Carboniferous Walton and Gays River deposits of southern Nova Scotia. The timing of mineralization is consistent with the previous estimates of ca. 300 Ma for other mineralization hosted by the Horton and Windsor groups in the Carboniferous of Nova Scotia.

La venue de Zn-Pb de Cheverie, à l'intérieur du bassin de Windsor dans le Sud de la Nouvelle-Écosse, est associée à l'altération carbonatée intense d'un dyke mafique et de schiste et siltstone déformés gris foncé voisins de la Formation carbonifère de Horton Bluff. Le dyke mafique, constitué de plagioclase automorphe (An<sub>45-60</sub>), de pyroxène augitique et d'ilménite comportant de la mésostasis et du granite porphyroïde de stade avancé, est subalcalin, affiche des affinités intra-plaque et est semblable aux BDMOE (basaltes de la dorsale médio-océanique enrichis); la structure chimique du clinopyroxène correspond à une structure chimique subalcaline-alkaline de transition. La datation (au <sup>40</sup>Ar/<sup>39</sup>Ar de la roche totale) du dyke mafique révèle que sa mise en place est survenue il y a 315 Ma, ce qui représente un âge minimal pour la déformation ductile des roches sédimentaires et un âge maximal pour la minéralisation.

La venue de pyrite, de marcasite, de sphalérite (pauvre en Fe et riche en Fe) et de galène conjuguée à du bitume est similaire à l'association métallique dans le gîte de métaux communs-baryte voisin de Walton et elle permet de supposer une affinité métallogénique. Les inclusions de fluides (L<sub>H<sub>2</sub>O</sub>-V) à deux phases dans le carbonate filonien s'homogénéisent entre 156° et 265 °C et ont des salinités de 0 à 22 ‰ en masse d'équivalent en NaCl. Les analyses des isotopes lourds révèlent: 1) des valeurs δ<sup>34</sup>S de –4,5 et de +2,2 ‰ de galène et de –4,4 ‰ de sphalérite; ainsi que 2) des valeurs δ<sup>13</sup>C de –8,8 et –1,4 ‰ de même que des valeurs δ<sup>18</sup>O de +22,5 et +21,2 ‰ de carbonate, cette dernière correspondant à une proportion de +11,7 à +13,0 ‰ à des températures de formation autour de 200 °C.

La composition chimique des fluides correspond aux fluides de bassin provenant de l'intérieur du bassin de Windsor et interagissant avec du pétrole liquide et d'autres fluides à faible salinité et basse température. Les chercheurs ont supposé un passé analogue dans le cas des fluides des gîtes carbonifères de Walton et de la rivière Gays dans le Sud de la Nouvelle-Écosse. Le moment de la minéralisation correspond aux datations estimatives antérieures d'environ 300 Ma d'autres minéralisations incluses dans le groupe de Horton-Windsor et remontant au Carbonifère en Nouvelle-Écosse.

Traduit par la rédaction

## INTRODUCTION

The basal Windsor Group of the Maritimes Basin hosts abundant base-metal mineralization, including the past-producing Gays River (Zn-Pb) and Walton (Ba-Zn-Pb-Cu-Ag) deposits of southern Nova Scotia. Although this mineralization has been examined in several geological investigations (e.g., Akande and Zentilli 1984; Ravenhurst *et al.* 1987 1989; Kontak 1992 1998; Chi *et al.* 1995; Chi and Savard 1996; Kontak and Sangster 1998), including a recent multi-disciplinary effort (Sangster and Savard 1998), many of the smaller occurrences remain poorly documented despite their relevance to broad-scale metallogeny. In this paper, the geology of a recently discovered small base-metal occurrence hosted by Horton Group rocks near Cheverie, Hants County (Fig. 1) is described and the implications for Carboniferous metallogenesis are discussed.

Mineralization at Cheverie, confined to rocks within an excavated gravel pit (Fig. 1c), consists of disseminated and fracture controlled Fe, Zn, Pb and Cu sulphide minerals associated with carbonate minerals, barite and liquid petroleum. Mineralization occurs in dark grey to black shale and siltstone of the Horton Bluff Formation and a mafic dyke. This particular area of mineralization is important because the association of mineralization with the mafic dyke permits assessment of the maximum age of mineralization via dating of the mafic dyke. The mafic dyke permits inferences regarding the tectonic setting based on whole-rock chemistry and the relative timing of deformation that affected the area. In addition, the element association (Ba, Mn, Zn, Pb, Cu; MacIssac 1998) and presence of liquid petroleum are features similar to the paragenesis documented at the nearby Walton barite-base metal deposit (Boyle 1972; Kontak and Sangster 1998).

## GEOLOGICAL SETTING

The Cheverie area lies in the Kennetcook Basin, one of several Carboniferous sub-basins within the large Maritimes Basin, which formed as a consequence of marine incursion following uplift and erosion related to the ca. 400 Ma Acadian Orogeny (see Calder (1998) for recent review). The oldest rocks are coarse clastics belonging to an unnamed member of the Horton Group. They rest unconformably on deformed and metamorphosed metaturbidite of the Meguma Group. The overlying rocks are grey to black, locally organic-rich siltstone and shale of the Horton Bluff Formation. Above this formation are red to grey arkose, sandstone, siltstone and conglomerate of the Cheverie Formation. They are overlain conformably by limestone, which belongs to the Macumber Formation of the Windsor Group, a thick marine succession dominated by carbonate and evaporite with minor fine-grained clastic intervals.

Rocks along the southern part of the Minas Basin (Noel Shore) locally record intense deformation related to periodic movement during the Carboniferous along the east-west trending Cobequid-Chedabucto Fault. For example, regional maps of the area produced by Stevenson (1959) and Boyle (1972) indicate areas of intense isoclinal folding and more detailed studies show similar structural complexities (e.g.,

Boehner 1991). More recently, the detailed work of Johnson (1999) in the Cheverie area has shown that this deformation is related to shallow thrusting of Middle Carboniferous age. The most recent regional mapping of the area indicates that in addition to the abundant folding, there is extensive faulting throughout the basin (Moore *et al.* 2000) that may have been important in terms of providing conduits for fluid migration.

The presence of mafic dykes cutting Horton Group sedimentary rocks in the area was noted by Boyle (1972), who discussed the dykes in the context of eruption of the Jurassic North Mountain Formation basalt. The latest mapping (Moore *et al.* 2000; and R.G. Moore, personal communication, 1998) indicates several more occurrences of dykes, including the one in the present study. Given the paucity of outcrop in much of the Kennetcook Basin, it is possible that the mafic dykes are more widespread than generally considered. To the knowledge of the authors, no previous absolute time constraints are available for any of these dykes.

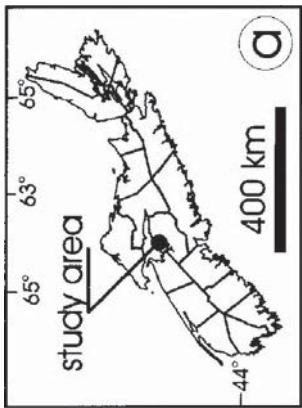
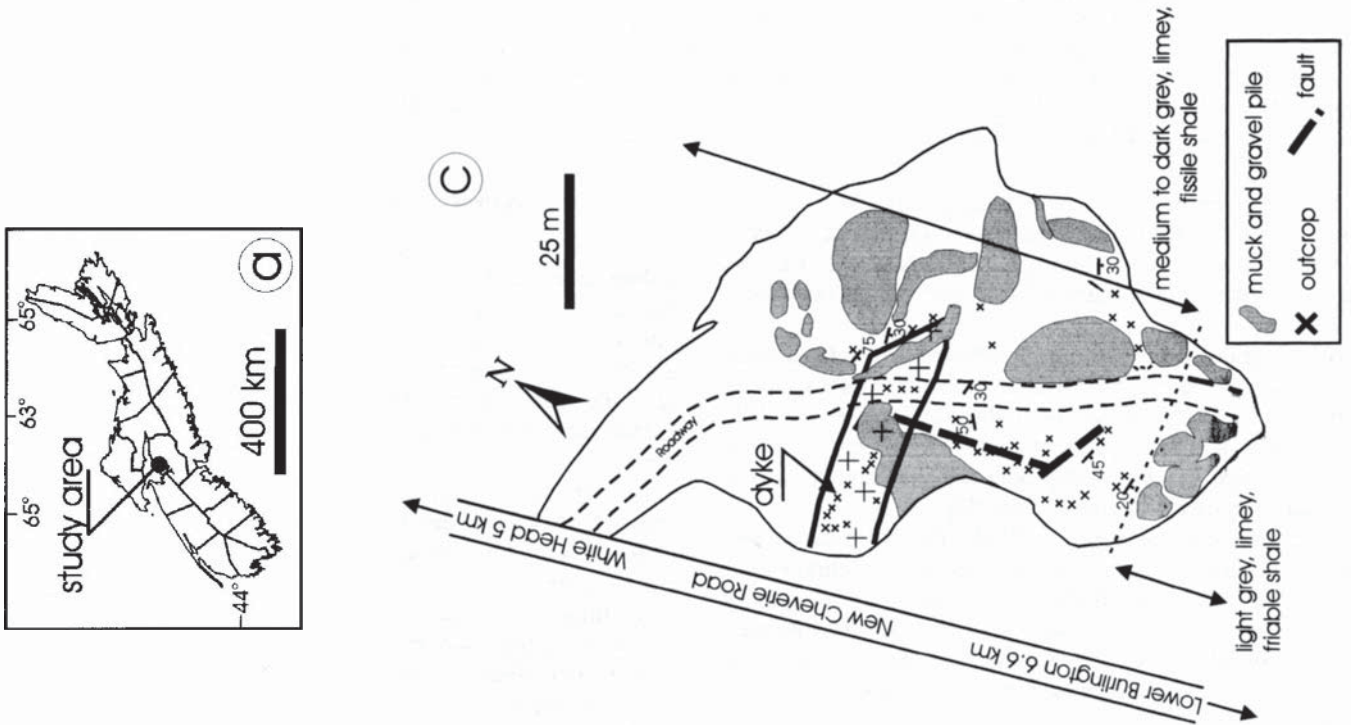
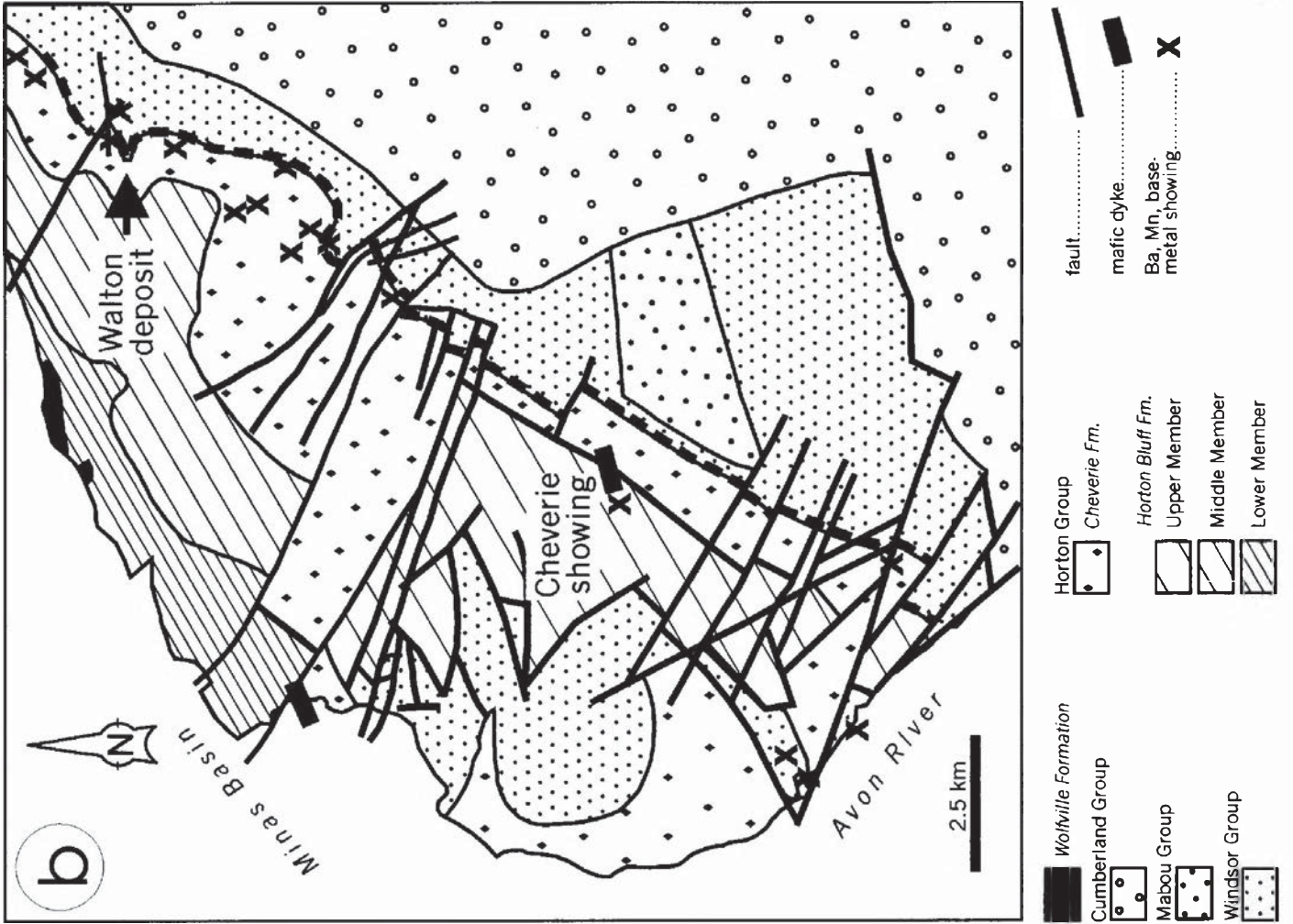
## GEOLOGY OF THE STUDY AREA AND NATURE OF HOST ROCKS AND MINERALIZATION

### Geology of the Cheverie showing

The mineralized area is exposed in an excavated pit just off the New Cheverie Road (Fig. 1c). The pit is underlain by pale to dark grey to black, finely bedded to fissile shale and siltstone that are assigned to the Horton Bluff Formation based on their features. This interpretation is consistent with the extent of this lithology in the surrounding area as mapped by Moore *et al.* (2000). The general stratigraphy exposed in the pit area consists of light-grey friable shale overlying medium to dark grey fissile shale. Fine-grained, alteration-related carbonate occurs within the sedimentary rocks. Locally the sedimentary rocks are intensely deformed with fold axes plunging 20–70° toward 185–210°. A penetrative fabric is lacking in the sedimentary rocks, but in thin section, boudinaging of coarser, relatively competent beds is observed, along with development of a ductile fabric (Fig. 2a, b). Locally the rocks are strongly fractured and the alignment of such outcrops within the pit area indicates that generally north-south and east-west faults transect the area.

The sedimentary rocks are cut by a northeast to east-west trending, ca. 10–12 m wide, dark green to black, fine-grained mafic dyke (Figs. 1c, 2a). The mafic dyke is variably altered and intensely fractured and brecciated on a local scale, possibly reflecting some fault movement. The margin of the dyke is noticeably finer grained than the plagioclase-phyric core. Variolitic textures characterize the dyke margin (Fig. 2d), suggesting that it was originally glassy. The dyke is

Fig. 1. (a) Outline of Nova Scotia showing the location of the study area. (b) Geological map of the central part of the Windsor or Kennetcook Basin with the location of the Cheverie showing (after Moore *et al.* 2000). Note that the showing is located near the contact of Horton Bluff Formation with the overlying Cheverie Formation. (c) Map of the Cheverie area showing outcrop distribution of sedimentary and dyke rock (after R. Mills, personal communication 2000).



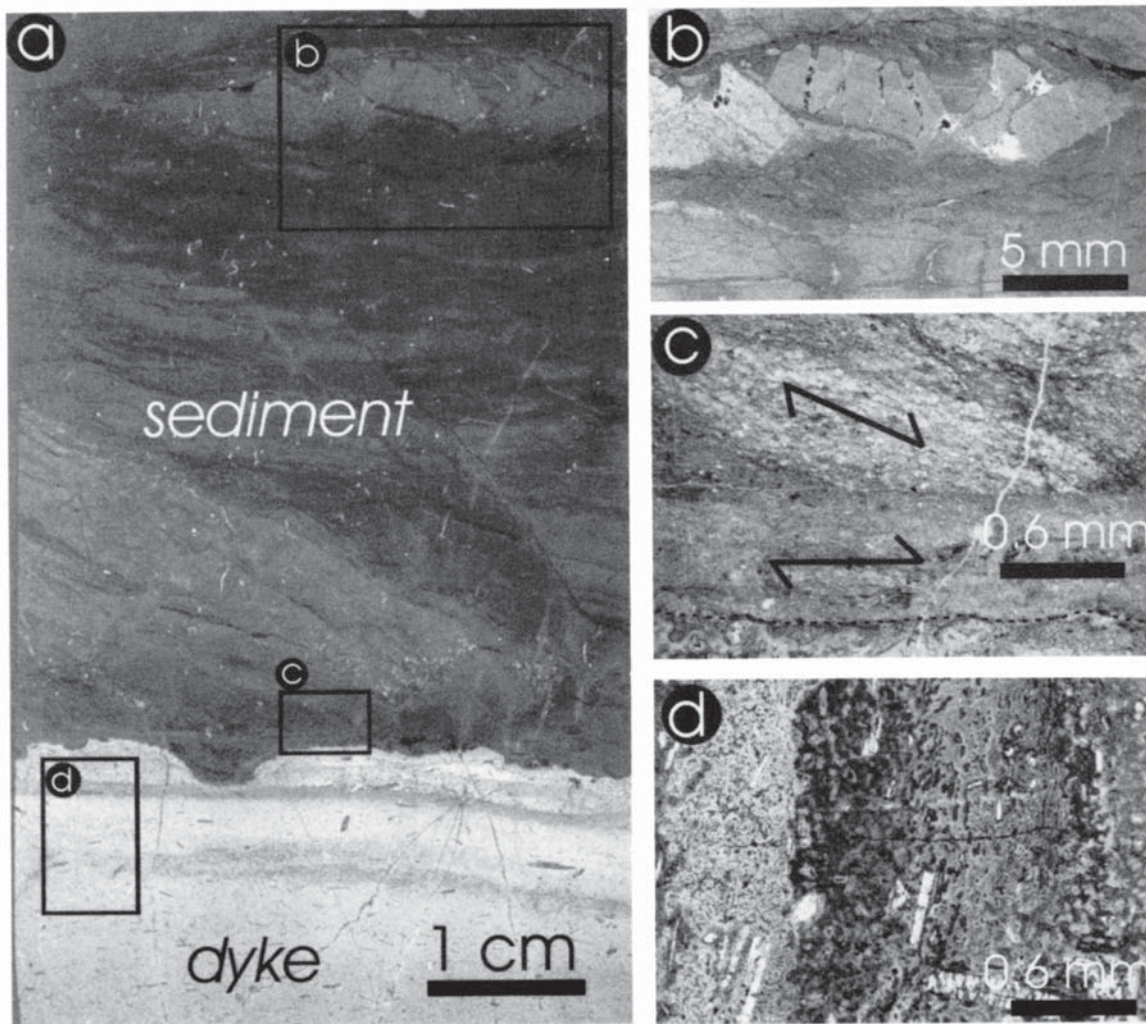


Fig. 2. Photomicrographs showing contact relationship between the dyke and host sedimentary rock. (a) Large thin section showing dyke rock and sediment. Note that the layering in the dyke rock reflects the presence of several zones formed at the contact as a result of chilling and subsequent devitrification. (b) Boudinaging of a relatively competent siltstone layer within more ductile shale. Note presence of extension cracks filled with carbonate. (c) Contact between host sedimentary rock and dyke (dotted black line at the base) showing ductile fabric in sedimentary rock that is oblique to the contact. Note that the fabric at the contact is within comminuted sedimentary rock and relates to subsequent brittle deformation. (d) Margin of mafic dyke showing development of variolitic texture in glassy matrix with minor amount of plagioclase microlites. Note that photo is rotated clockwise 90° compared to Fig. 2a.

variably fractured with an orthogonal pattern developed in places, and some fracture surfaces have slickensides. Rusty-brown carbonate with minor quartz coats some fracture surfaces and the dyke is bleached to a buff colour near these fractures.

Examination of the dyke-host sedimentary rock contacts (Fig. 2) indicates the presence of a penetrative fabric in the sedimentary rocks that is oblique to the contact (Fig. 2c). This early, ductile fabric is post-dated by a subsequent brittle deformation that has brecciated both the host and dyke; the related fabric is parallel to the contact (Fig. 2c).

Mineralization, including sulphide minerals, carbonate, barite and quartz as veins and replacements, occurs within both the host rock and mafic dyke and is predominantly fracture controlled, but lesser amounts of disseminated mineralization also occurs. The mineralization is confined to the area of outcrop within the excavated pit shown in Fig. 1c.

#### Mineralization, alteration, and paragenesis

Mineralization consists of pyrite, marcasite, sphalerite and galena associated with white to brown carbonate, barite and quartz in veins and coating fractures (paragenesis in Fig. 3). All phases are finely crystalline and subhedral to anhedral. Hand samples containing visible mineralization have assayed at 5,700 ppm Pb and 76,000 ppm Zn, with no Ag or Au (MacIssac 1998; and J. MacIssac, personal communication, 1998).

Alteration envelopes several cm wide are visible around internally banded veins (Fig. 4c). The altered sedimentary and dyke rocks are buff coloured. The veins with widths of several cm have an internal texture indicative of repetitive opening and filling; for example, comb-textured veins containing abundant calcite euhedra (Fig. 4e, f) and intricate banding of quartz and carbonate. The margin of the mafic dyke or contact zone with the host may be brecciated, thus brittle deformation of the rocks was pre- or syn-mineralization and alteration. In

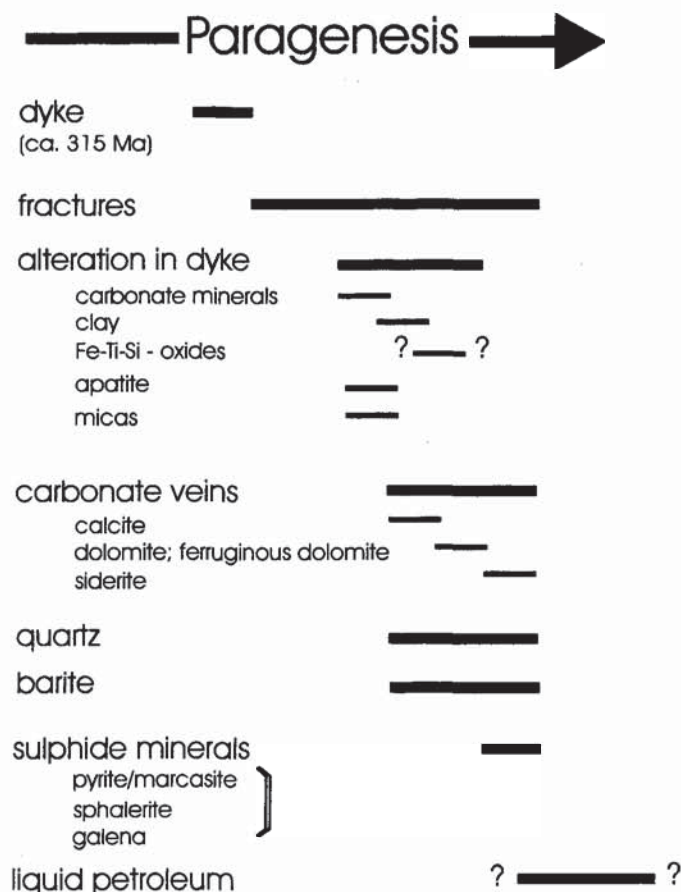


Fig. 3. Paragenesis of vein mineralogy and alteration for the Cheverie showing. Note that the diagram is a summary of observations from both petrographic (hand samples and thin sections) and imaging (e.g., Figs. 4, 5) analysis.

some cases, altered wall-rock material occurs as fragments within irregular veinlets filled by gangue minerals. Altered mafic dyke is locally coated by a white clay mineral.

In general, the veins are 1–2 cm wide and contain, in decreasing order of abundance, finely crystalline quartz, carbonate and barite. Sulphide minerals form a minor component of the veins except where they occur as fracture coatings. The veins may occur as multiple sets of subparallel veinlets or show mutually crosscutting relationships. Internally the veins are massive and, as noted above, may be laminated with fibre or comb textures (Fig. 4d, e).

Pyrite occurs as massive, anhedral to euhedral crystals coating fracture surfaces or disseminated within altered sedimentary and dyke rock, where carbonate is abundant. Marcasite occurs as spheroidal aggregates intergrown with white carbonate surrounded by light brown or buff carbonate (Fig. 4b). The detailed relationship between the various Fe sulphide minerals is unknown.

Galena occurs at the contact between veins and wall rock material and is commonly intergrown with carbonate, as inclusion-free crystals (Fig. 4c).

Alteration of the host and dyke rocks proximal to fractures and veins (Fig. 4a, c, d) is evident as buff discoloration due to replacement of the matrix by Fe-rich carbonate and silica. The fine-grained nature of the

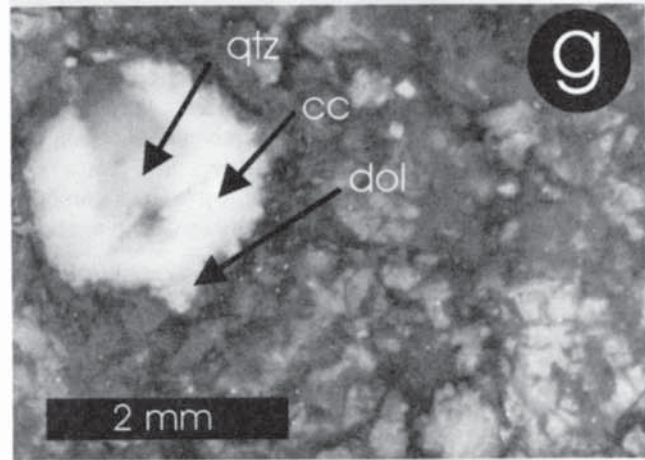
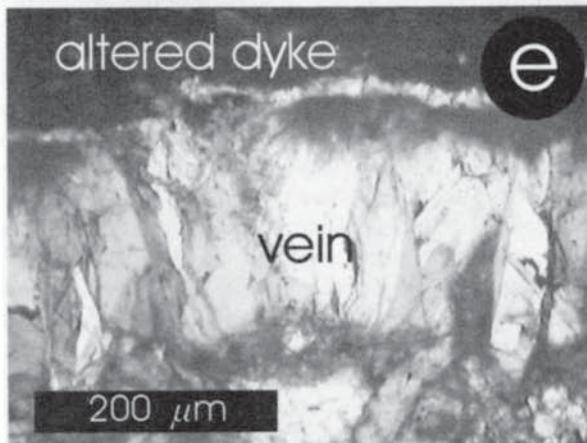
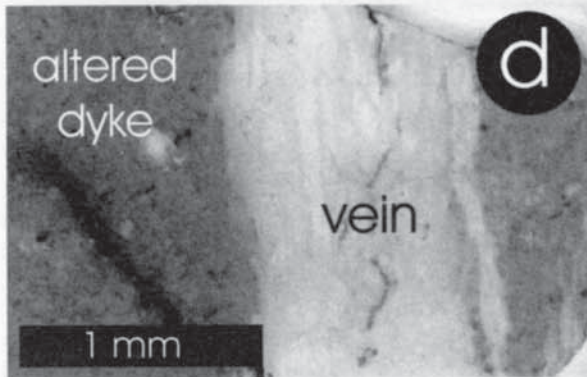
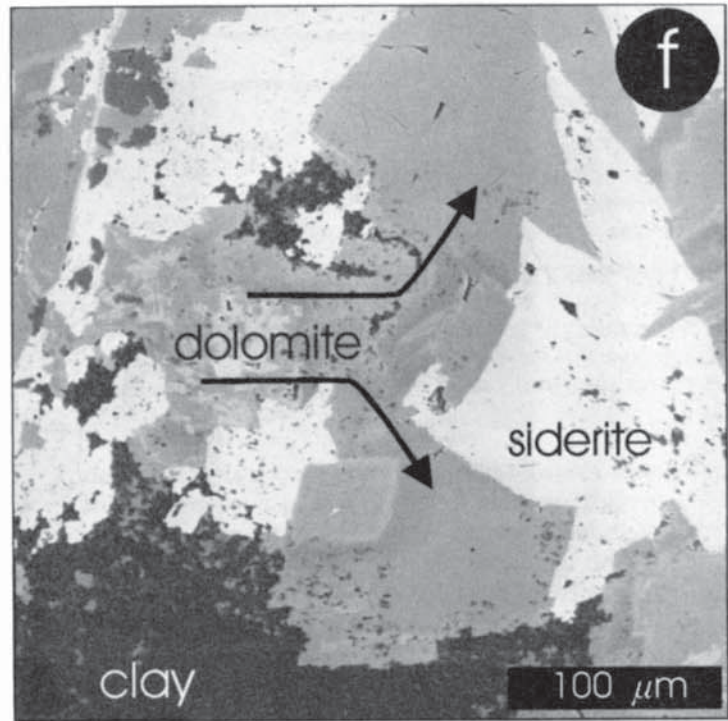
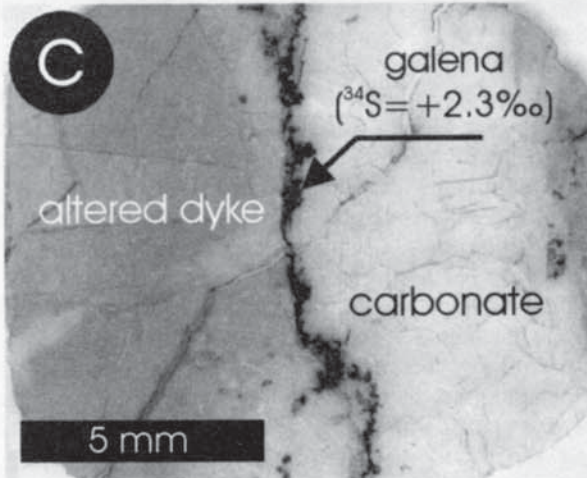
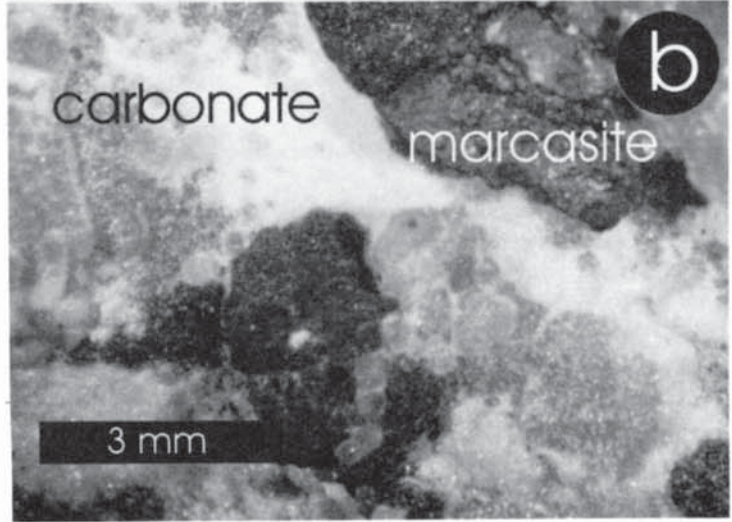
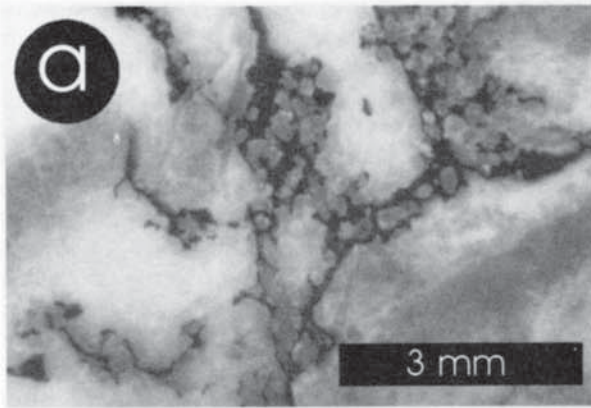
sedimentary rocks precludes detailed observations of the alteration. The alteration is more easily seen in the dyke rock due to its coarser texture and reactive nature. In thin section, the mafic dyke is seen to be intensely carbonatized with additional minerals including quartz, biotite, chlorite, clay, apatite and Fe-Ti oxides (Fig. 5). Carbonate occurs as fine crystals and disseminations obliterating the original rock texture. It also occurs as intergranular material between apparently fresh plagioclase euhedra (Fig. 5c); imaging analysis indicates that this carbonate is of variable composition (Figs. 4f, 5h, i). The carbonate incorporates irregular patches of clay material (Fig. 4f) and is also crosscut by veinlets of the same material. Alteration of the mafic dyke is very heterogeneous, with pervasive versus localized alteration present. Textures of secondary Fe-Ti-Si oxide phases (compositions discussed below) suggest pseudomorphing of primary oxide phases (Fig. 5g). Fine-grained biotite and chlorite occur as irregular masses within the carbonate assemblage (Fig. 5e). Apatite grains in the carbonate assemblage suggest that apatite is part of the alteration assemblage. Finally, quartz occurs as anhedral patches intergrown with zoned carbonate minerals (Fig. 4g).

A soft, black substance, probably liquid petroleum and bitumen, fills pores (Fig. 4a) and coats fractures. The petroleum has not been observed as inclusions within any of the hydrothermal phases. Thus, its migration appears to be late relative to the alteration and mineralization.

In summary, the paragenesis for the mineralization and alteration indicates that structural preparation pre-dated and was synchronous with infiltration of the mineralizing and altering fluids and that this event was syn- or post-dyke emplacement (ca. 315 Ma, see below).

#### ANALYTICAL PROCEDURES

Whole-rock samples of dyke material were dated by the  $^{40}\text{Ar}/^{39}\text{Ar}$  technique using a laser step-wise heating method at Queen's University, Kingston, Ontario using the procedures of Clark *et al.* (1998). Errors given are  $2\sigma$  and do not incorporate the error in the J value (Table 1). Whole-rock major- and trace-element analyses of the dyke were obtained by XRF at the regional geochemical facility at St. Mary's University, Halifax, Nova Scotia. Trace elements and rare-earth elements were obtained by solution ICP-MS at Memorial University, St. John's, Newfoundland (Jenner *et al.* 1990). The  $\text{CO}_2$  analyses were done at DalTech, Halifax. Mineral chemistry was obtained using a JEOL Superprobe at Dalhousie University, Halifax with the following operating conditions: 1–10  $\mu\text{m}$  beam diameter, 15 kV accelerating voltage, 5 nA beam current. Detailed imaging was also done on the electron microprobe and these results are shown here as back-scattered electron images. Sulphur isotopic analysis of galena and sphalerite separates were obtained at the University of Saskatchewan, following procedures in Kontak *et al.* (1999), and carbon and oxygen isotopic analysis of carbonate were done at the same university following procedures in Kontak and Kerrich (1997). The results are reported in the standard  $\delta$  notation relative to Canyon Diablo troilite (CDT) for sulphur, Vienna Standard Mean Ocean Water (V-SMOW) for oxygen and Pee Dee belemnite (PDB) for carbon. Analysis of



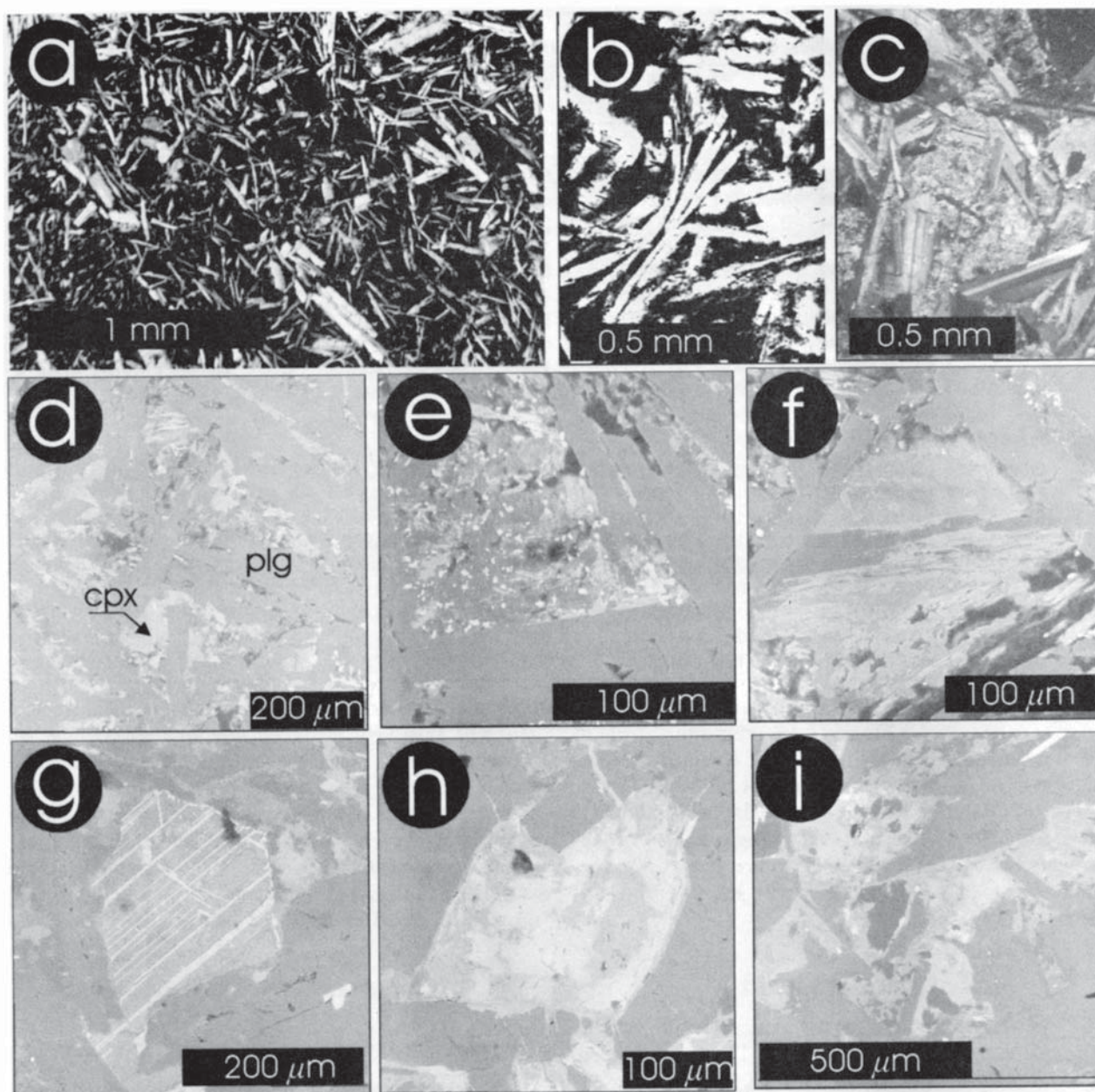


Fig. 5. Photomicrographs (a, b, c) and back scattered electron (BSE) images (d to i) of mafic dyke and related alteration at Cheverie showing. (a) Plane-polarized light photo of trachytic texture within dyke. The intergranular material consists of clinopyroxene and alteration products. (b) Close up of dyke matrix in plane light showing the plagioclase laths and intergranular material dominated by finely crystalline clinopyroxene, skeletal opaques, and alteration minerals. (c) Cross-polars photomicrograph of dyke with abundant intergranular carbonate after matrix material (former glass?). The remnant plagioclase is fresh despite the abundance of carbonate. (d) BSE image of dyke sample showing tabular plagioclase (plg), equant to acicular clinopyroxene (cpx) and intergranular clinopyroxene, opaques and alteration minerals (i.e., carbonate, mica, opaques). (e, f) Close up BSE images of intergranular material showing disseminated opaques, fine-grained clinopyroxene and mixed silicates (feldspar, carbonate, mica, clay). These areas may represent crystallization and later alteration of glass. (g) BSE image showing outline of primary Fe-Ti oxide with exsolution lamellae. The crystal has subsequently been altered to a complex mixture of Fe-Ti-Si minerals. (h, i) BSE images showing mixed carbonate phases (bright areas Fe-rich) developed at the expense of pre-existing clinopyroxene and matrix material.

Fig. 4. Photographs of rocks and polished thin-section material from the Cheverie showing. (a) Paragenetically late carbonate (white) invades altered mafic dyke (dark grey material). The dark material in the veinlets is bitumen. (b) Carbonate minerals (calcite, dolomite, Fe-Mg calcite) infilling porosity in fractured dyke with late-stage marcasite. (c) Altered mafic dyke cut by vein carbonate with galena mineralization at the boundary. This galena was sampled for sulphur isotopic analysis, as indicated. (d) Laminated vein in altered dyke with textures reflecting multiple extensional events. (e) Part of laminated vein shown in Fig. 4d showing comb-textured carbonate crystals growing inwards from the wall of altered dyke rock. (f) Back scattered electron image of altered dyke with siderite, dolomite and ferruginous dolomite and clay mineral. (g) Altered dyke with ovoid occluded by quartz and later carbonate phases (qtz=quartz, cc=calcite, dol=dolomite).

Table 1. Ar-Ar data for mafic dyke samples, Cheverie showing, Nova Scotia.

| Laser Power (W)                                   | $^{36}\text{Ar}/^{40}\text{Ar}$<br>( $\pm 2\sigma$ ) | $^{39}\text{Ar}/^{40}\text{Ar}$<br>( $\pm 2\sigma$ ) | Ca/K    | Cl/K  | % $^{40}\text{Ar}$<br>Atm. | % $^{39}\text{Ar}$<br>of total | $^{40}\text{Ar}^*/^{39}\text{Ar}_K$<br>( $\pm 2\sigma$ ) | Age<br>(Ma, $\pm 2\sigma$ ) |
|---|--|--|---------|-------|----------------------------|--------------------------------|--|-----------------------------|
| Sample MI-96-6, J value = 0.007988 $\pm$ 0.000048 |  |  |         |       |                            |                                |  |                             |
| 0.50  | 0.00253843 $\pm$ 0.00079959                          | 0.021882 $\pm$ 0.002023                              | 15.587  | 0.058 | 74.87                      | 3.70                           | 11.464 $\pm$ 1.381                                       | 158.0 $\pm$ 18.2            |
| 1.00  | 0.00154842 $\pm$ 0.00040786                          | 0.031711 $\pm$ 0.001053                              | 21.858  | 0.043 | 45.61                      | 9.15                           | 17.139 $\pm$ 0.650                                       | 231.4 $\pm$ 8.2             |
| 1.50  | 0.00067119 $\pm$ 0.00021494                          | 0.035009 $\pm$ 0.000584                              | 13.586  | 0.050 | 19.68                      | 16.95                          | 22.937 $\pm$ 0.470                                       | 303.5 $\pm$ 5.7             |
| 2.00  | 0.00025919 $\pm$ 0.00018421                          | 0.036235 $\pm$ 0.000522                              | 6.164   | 0.071 | 7.46                       | 22.91                          | 25.537 $\pm$ 0.318                                       | 334.9 $\pm$ 3.8             |
| 2.25  | 0.00046887 $\pm$ 0.00031030                          | 0.036839 $\pm$ 0.000865                              | 5.564   | 0.074 | 13.64                      | 9.18                           | 23.440 $\pm$ 0.649                                       | 309.6 $\pm$ 7.8             |
| 2.50  | 0.00038675 $\pm$ 0.00035299                          | 0.036776 $\pm$ 0.000963                              | 7.424   | 0.077 | 11.20                      | 9.16                           | 24.142 $\pm$ 0.553                                       | 318.1 $\pm$ 6.6             |
| 2.75  | 0.00040193 $\pm$ 0.00070590                          | 0.037591 $\pm$ 0.001816                              | 12.288  | 0.081 | 11.63                      | 4.42                           | 23.504 $\pm$ 1.232                                       | 310.4 $\pm$ 14.9            |
| 3.75  | 0.00034050 $\pm$ 0.00034947                          | 0.037322 $\pm$ 0.000961                              | 12.437  | 0.086 | 9.81                       | 9.49                           | 24.163 $\pm$ 0.612                                       | 318.3 $\pm$ 7.3             |
| 5.25  | 0.00044607 $\pm$ 0.00075410                          | 0.037222 $\pm$ 0.001927                              | 26.142  | 0.089 | 12.92                      | 4.75                           | 23.391 $\pm$ 1.376                                       | 309.0 $\pm$ 16.7            |
| 7.00  | 0.00051583 $\pm$ 0.00038682                          | 0.035023 $\pm$ 0.001048                              | 39.956  | 0.062 | 15.06                      | 10.29                          | 24.247 $\pm$ 0.614                                       | 319.4 $\pm$ 7.4             |
| Sample MI-96-7 J value = 0.007995 $\pm$ 0.000048  |  |  |         |       |                            |                                |  |                             |
| 0.75  | 0.00318566 $\pm$ 0.00225868                          | 0.014320 $\pm$ 0.005703                              | 111.409 | 0.225 | 93.85                      | 5.92                           | 4.263 $\pm$ 4.284  | 60.4 $\pm$ 59.7             |
| 1.00  | 0.00322544 $\pm$ 0.00202651                          | 0.030745 $\pm$ 0.005063                              | 106.492 | 0.066 | 95.07                      | 6.49                           | 1.575 $\pm$ 3.937  | 22.5 $\pm$ 56.0             |
| 1.50  | 0.00208968 $\pm$ 0.00104303                          | 0.033171 $\pm$ 0.002609                              | 51.898  | 0.037 | 61.60                      | 13.07                          | 11.559 $\pm$ 2.215                                       | 159.4 $\pm$ 29.2            |
| 1.75  | 0.00232927 $\pm$ 0.00176874                          | 0.035791 $\pm$ 0.004391                              | 46.338  | 0.038 | 68.65                      | 7.22                           | 8.737 $\pm$ 3.812  | 121.8 $\pm$ 51.3            |
| 2.00  | 0.00030566 $\pm$ 0.00117176                          | 0.035206 $\pm$ 0.002949                              | 26.859  | 0.034 | 8.93                       | 8.42                           | 25.864 $\pm$ 2.079                                       | 339.0 $\pm$ 24.8            |
| 2.50  | 0.00043289 $\pm$ 0.00136291                          | 0.034317 $\pm$ 0.003408                              | 23.016  | 0.052 | 12.64                      | 7.59                           | 25.451 $\pm$ 2.529                                       | 334.1 $\pm$ 30.3            |
| 3.00  | 0.00048137 $\pm$ 0.00193163                          | 0.033100 $\pm$ 0.004806                              | 23.318  | 0.078 | 14.02                      | 5.50                           | 25.973 $\pm$ 4.043                                       | 340.4 $\pm$ 48.2            |
| 4.50  | 0.00062755 $\pm$ 0.00178444                          | 0.031031 $\pm$ 0.004485                              | 23.893  | 0.097 | 18.30                      | 5.84                           | 26.323 $\pm$ 3.068                                       | 344.5 $\pm$ 36.5            |
| 7.00  | 0.00059771 $\pm$ 0.00029782                          | 0.027139 $\pm$ 0.000770                              | 31.368  | 0.073 | 17.50                      | 39.94                          | 30.394 $\pm$ 0.601                                       | 392.4 $\pm$ 6.9             |

laboratory standards indicates that reproducibility ( $1\sigma$ ) of  $\delta^{34}\text{S}$ ,  $\delta^{18}\text{O}$  and  $\delta^{13}\text{C}$  to be 0.3‰, 0.2‰ and 0.1‰, respectively. Fluid inclusion thermometric measurements were obtained using a Fluid Inc. gas-flow heating/freezing stage at the Nova Scotia Department of Natural Resources in Halifax following procedures described by Kontak (1998). The precision of the measurements is  $\pm 0.2^\circ\text{C}$  for low-temperature and  $\pm 1.0^\circ\text{C}$  for high-temperature phase changes, as estimated from measurements of standards.

#### AGE OF THE MAFIC DYKE

Two  $^{40}\text{Ar}/^{39}\text{Ar}$  age spectra for the mafic dyke are shown in Fig. 6 and data are given in Table 1. The spectrum for sample MI-96-6 shows a monotonic increase in age from an initial, low-temperature step of ca. 160 Ma to a plateau age of  $315 \pm 4$  Ma for the last 6 steps, which incorporate 47% of the gas. The Ca/K ratios (Table 1) define a saddle-type pattern indicating liberation of gas from different sites (i.e., mineral phases) and there is no consistent correlation with the apparent ages for steps. The shape of the age spectrum suggests partial resetting with loss of ca. 5–10% of its gas (Turner 1968; McDougall and Harrison 1988). The second age spectrum, for sample MI-96-7, consists of two contrasting profiles. The low-temperature steps are characterized by young ages with high associated errors due to the low K content (Ca/K ratios of 111 to 46) and high atmospheric contribution (95 to 61 %). In contrast, the higher-temperature steps indicate that older apparent ages and one four-step segment incorporating 28% of the gas defines a plateau age of  $339 \pm 17$  Ma. These higher temperature steps are characterized by lower atmospheric gas (8 to 18%) and lower Ca/K ratios (23 to 26).

Given the undeformed nature of the mafic dyke and lack of intense alteration in MI-96-6, the plateau age defined by the high-temperature steps for this sample probably represents the

time of emplacement and crystallization of the dyke at ca. 315 Ma. The relatively disturbed spectrum for sample MI-96-7 probably relates to the presence of considerable alteration within the intergranular matrix of this sample. The low-temperature steps in both samples reflect a later, mild thermal overprinting event during the Jurassic or later time (McDougall and Harrison 1988). The integrated ages for the samples of 305 and 290 Ma are not considered geologically meaningful given the shapes of the age spectra and loss of gas.

#### PETROLOGY OF THE MAFIC DYKE

##### Petrography and mineral chemistry of primary phases

Several samples of the mafic dyke examined in thin section reveal uniform mineralogical and textural features, but as noted previously, the margin is characterized by a narrow zone (i.e., few cm) of devitrified glass. The core of the mafic dyke is dominated (i.e., 60–70%) by normally zoned, inclusion-free, euhedral plagioclase (0.2–0.5 mm) laths that define a trachytic texture. Plagioclase is intergrown with finer-grained clinopyroxene euhedra (Fig. 5a, b, c, d). Rare quartz-feldspar intergrowths define a granophyric-like texture in the intergranular areas, reflecting late-stage evolution of the magma to a felsic composition. A varied assemblage of mixed carbonate, serpentine minerals, chlorite, biotite and leucoxene aggregates, with carbonate minerals being the most abundant (Fig. 5c, e) also occurs interstitially. The texture in some areas suggests that alteration may have replaced intergranular glass. The opaque phase is ilmenite, which occurs as acicular or skeletal laths or equant grains.

Plagioclase laths are uniform in composition with core and rims of  $\text{An}_{45-60}$ , but more sodic compositions occur in the intergranular areas ( $\text{An}_{13-30}$ ; Table 2, Fig. 7a). Clinopyroxene



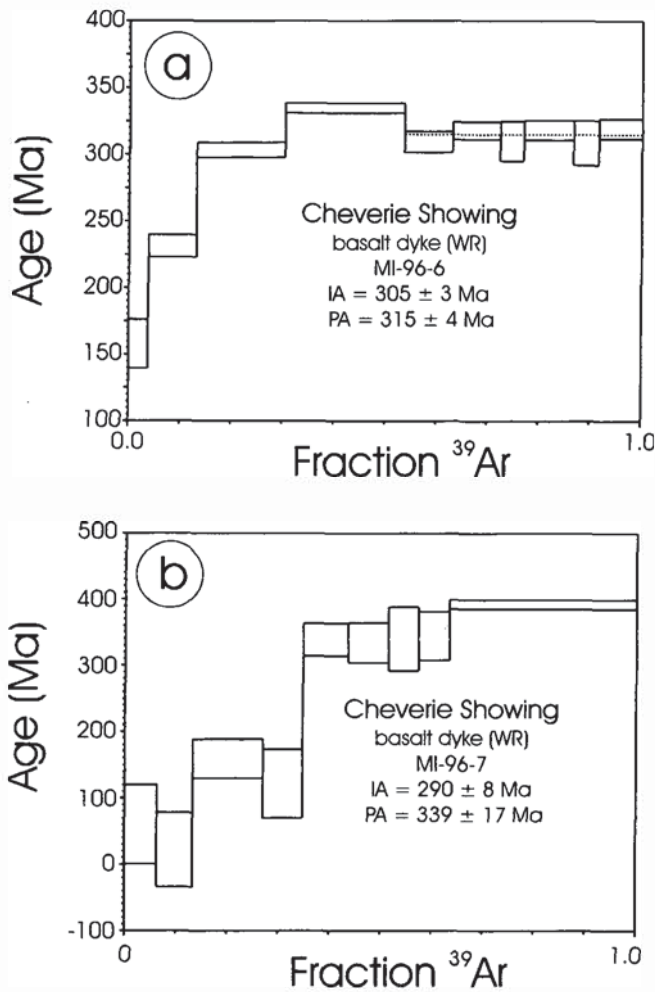


Fig. 6. Conventional  $^{40}\text{Ar}/^{39}\text{Ar}$  age spectra plots for whole rock samples (WR) of mafic dyke from Cheverie showing. The abbreviations are: IA = integrated age, and PA = plateau age. (a) MI-96-6 sample with a plateau age of 315 Ma, as defined by the high-temperature fraction, with the low-temperature fraction indicating a thermal overprint at ca. 160 Ma. (b) MI-96-7 sample with a poorly defined plateau age of 339 Ma, as defined by the high-temperature fraction, with the low-temperature fraction indicating a poorly defined thermal overprinting event.

is of augite composition (Fig. 7b) and is characterized by elevated titanium contents (2–3 wt. %  $\text{TiO}_2$ , Table 2), which is typical of clinopyroxene in alkali basalts. The opaque phase is ilmenite (Fig. 7c) and imaging indicates that primary textures such as exsolution are lacking, although such textures occur as secondary features, as noted above. Coarse apatite needles are uniform in composition with Mn the only detectable minor element (0.1 to 0.2 wt. % MnO). Rare vestiges of partially chloritized biotite occur ( $\text{Fe}/(\text{Fe}+\text{Mg}) = 0.2\text{--}0.62$ ; Table 2). There is neither primary olivine nor alteration products of it present.

#### Alteration Mineralogy

Alteration minerals in the mafic dyke include clay, chlorite, carbonate minerals and mixed Fe-Ti-Si phases as pseudomorphs of a primary oxide phase. The clay mineral (Table 2) is suspected to be kaolinite. Secondary chlorite is

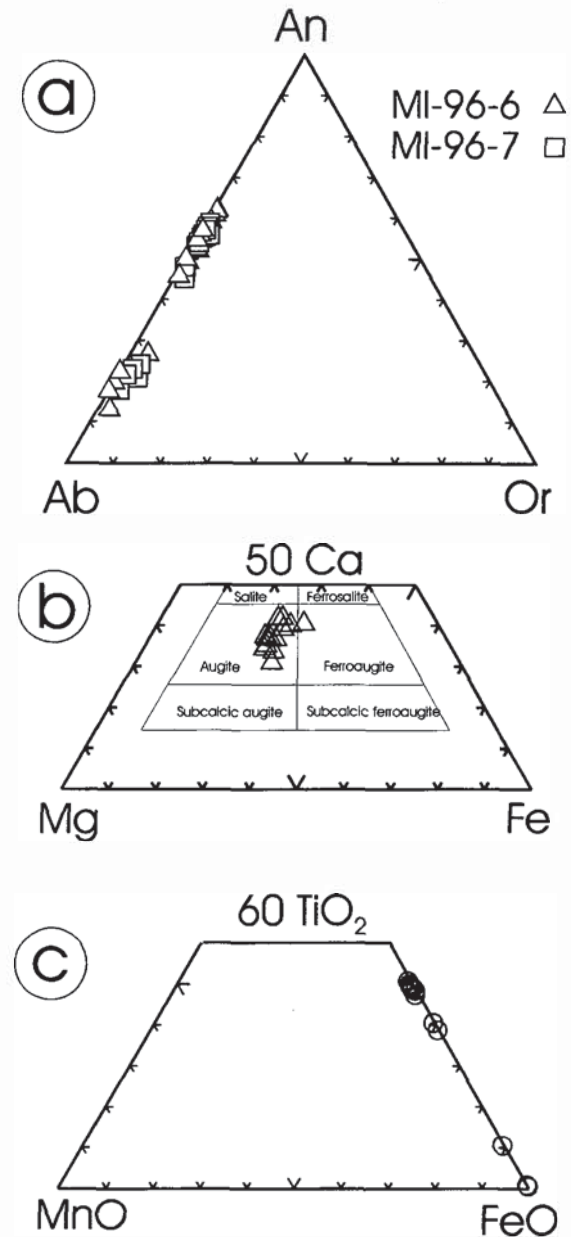


Fig. 7. Mineral chemistry for the mafic dyke from the Cheverie showing. (a) Ternary An-Ab-Or plot for plagioclase showing compositions in the range  $\text{An}_{45-60}$  for coarse laths and more sodic compositions ( $\text{An}_{12-30}$ ) for the late-stage, quartz-feldspar granophyre and altered plagioclase. (b) Ternary Mg-Ca-Fe plot for pyroxene indicating an augitic composition. (c) Ternary MnO- $\text{TiO}_2$ -FeO plot for opaque phases.

uniform in composition ( $\text{Fe}/(\text{Fe}+\text{Mg}) = 0.45\text{--}0.55$ ), but trace amounts of  $\text{K}_2\text{O}$  (to 2–3 wt. %) and  $\text{TiO}_2$  (to 1.0 wt. %) in some analyses reflect incomplete replacement of biotite. Carbonate occurs as disseminated patches and isolated crystals within the mafic dyke and has a complex chemistry. Based on imaging (Figs. 4f, 5h, i) and point analysis (Table 3), it appears that carbonate paragenesis is consistently calcite, ferroan dolomite/ankerite and magnesian siderite. The range in carbonate compositions is summarized in Fig. 8. Ilmenite, the primary oxide phase, has been altered to a mixed assemblage of Fe-Ti-Si phases (Fig. 7c).

Table 2. Representative electron microprobe analysis (in wt. %) for silicates, Cheverie showing, Nova Scotia.

| Sample Mineral                 | MI-96-6 cpx core | MI-96-6 cpx rim | MI-96-6 cpx core | MI-96-6 cpx mat. | MI-96-6 cpx mat. | MI-96-6 plg core | MI-96-6 plg core | MI-96-6 plg rim | MI-96-7 plg core | MI-96-7 plg core | MI-96-7 plg core | MI-96-7 biotite | MI-96-7 chlorite | MI-96-1 clay | MI-96-1 clay |
|--------------------------------|------------------|-----------------|------------------|------------------|------------------|------------------|------------------|-----------------|------------------|------------------|------------------|-----------------|------------------|--------------|--------------|
| SiO <sub>2</sub>               | 47.34            | 47.25           | 47.33            | 48.49            | 48.49            | 53.99            | 52.18            | 57.22           | 64.38            | 53.50            | 56.61            | 35.28           | 30.75            | 46.06        | 47.04        |
| TiO <sub>2</sub>               | 2.12             | 2.41            | 1.92             | 1.85             | 1.85             | 0.00             | 0.00             | 0.00            | 0.00             | 0.00             | 0.00             | 2.87            | 0.00             | 0.00         | 0.00         |
| Al <sub>2</sub> O <sub>3</sub> | 3.39             | 3.14            | 3.57             | 2.77             | 2.77             | 27.64            | 28.94            | 24.92           | 22.47            | 28.99            | 27.15            | 11.70           | 11.20            | 38.08        | 38.67        |
| FeO                            | 15.63            | 15.34           | 15.14            | 17.12            | 17.12            | 0.00             | 0.00             | 0.00            | 0.00             | 0.00             | 0.00             | 22.06           | 24.94            | 0.00         | 0.00         |
| MnO                            | 0.25             | 0.25            | 0.19             | 0.41             | 0.41             | 0.00             | 0.00             | 0.00            | 0.00             | 0.00             | 0.00             | 0.00            | 0.00             | 0.00         | 0.00         |
| MgO                            | 12.95            | 10.21           | 10.59            | 12.43            | 12.43            | 0.00             | 0.00             | 0.00            | 0.00             | 0.00             | 0.00             | 11.15           | 17.38            | 0.00         | 0.00         |
| CaO                            | 16.30            | 19.32           | 19.51            | 16.03            | 16.03            | 11.21            | 12.61            | 8.43            | 3.90             | 12.10            | 9.68             | 0.00            | 0.00             | 0.00         | 0.00         |
| Na <sub>2</sub> O              | 0.48             | 0.52            | 0.65             | 0.54             | 0.54             | 5.07             | 4.43             | 5.66            | 7.61             | 4.79             | 5.92             | 0.00            | 0.00             | 0.00         | 0.00         |
| K <sub>2</sub> O               | 0.00             | 0.02            | 0.00             | 0.00             | 0.00             | 0.11             | 0.07             | 0.29            | 0.73             | 0.15             | 0.24             | 7.29            | 0.00             | 0.00         | 0.00         |
| Total                          | 98.46            | 98.46           | 98.90            | 99.65            | 99.65            | 98.02            | 98.23            | 96.52           | 99.09            | 99.53            | 99.60            | 90.35           | 84.27            | 84.14        | 85.71        |

## Structural Formulae

| Number O | 6     | 6     | 6     | 6     | 6     | 8    | 8    | 8    | 8    | 8    | 8    | 22   | 28   | 20   | 20   |
|----------|-------|-------|-------|-------|-------|------|------|------|------|------|------|------|------|------|------|
| Si       | 11.05 | 11.12 | 11.09 | 11.23 | 11.23 | 2.45 | 2.37 | 2.63 | 2.85 | 2.42 | 2.54 | 5.68 | 6.72 | 6.89 | 6.89 |
| Al       | 0.94  | 0.86  | 0.97  | 0.76  | 0.76  | 1.48 | 1.55 | 1.35 | 1.17 | 1.55 | 1.44 | 0.81 | 2.88 | 6.72 | 6.67 |
| Ti       | 0.36  | 0.43  | 0.32  | 0.32  | 0.32  | 0.00 | 0.00 | 0.00 | 0.00 | 0.00 | 0.00 | 0.13 | 0.00 | 0.00 | 0.00 |
| Fe       | 3.06  | 3.02  | 2.95  | 3.31  | 3.31  | 0.00 | 0.00 | 0.00 | 0.00 | 0.00 | 0.00 | 1.08 | 4.56 | 0.00 | 0.00 |
| Mn       | 0.00  | 0.00  | 0.00  | 0.07  | 0.07  | 0.00 | 0.00 | 0.00 | 0.00 | 0.00 | 0.00 | 0.00 | 5.66 | 0.00 | 0.00 |
| Mg       | 4.50  | 3.56  | 3.71  | 4.28  | 4.28  | 0.00 | 0.00 | 0.00 | 0.00 | 0.00 | 0.00 | 0.98 | 0.00 | 0.00 | 0.00 |
| Ca       | 4.07  | 4.86  | 4.90  | 3.96  | 3.96  | 0.54 | 0.62 | 0.42 | 0.18 | 0.59 | 0.46 | 0.00 | 0.00 | 0.00 | 0.00 |
| Na       | 0.00  | 0.00  | 0.00  | 0.00  | 0.00  | 0.45 | 0.39 | 0.50 | 0.66 | 0.42 | 0.51 | 0.00 | 0.00 | 0.00 | 0.00 |
| K        | 0.00  | 0.00  | 0.00  | 0.00  | 0.00  | 0.01 | 0.00 | 0.02 | 0.04 | 0.01 | 0.02 | 0.54 | 0.00 | 0.00 | 0.00 |

Table 3. Representative electron microprobe analysis (in wt. %) for carbonate minerals, Cheverie showing, Nova Scotia.

| Sample Point | MI-96-6 13 | MI-96-6 16 | MI-96-6 17 | MI-96-6 18 | MI-96-6 27 | MI-96-1 1 | MI-96-1 7 | MI-96-1 9 | MI-96-7 7 | MI-96-7 8 | MI-96-7 9 | MI-96-7 14 | MI-96-7 15 | MI-96-7 16 | MI-96-7 17 | MI-96-7 18 |
|--------------|------------|------------|------------|------------|------------|-----------|-----------|-----------|-----------|-----------|-----------|------------|------------|------------|------------|------------|
| FeO          | 37.04      | 36.57      | 42.49      | 5.23       | 33.38      | 12.14     | 0.00      | 0.55      | 38.77     | 6.11      | 39.07     | 43.34      | 35.77      | 31.37      | 10.49      | 29.79      |
| MnO          | 0.92       | 0.78       | 1.83       | 1.66       | 0.70       | 0.35      | 1.19      | 0.98      | 3.35      | 1.42      | 4.02      | 0.74       | 0.64       | 0.60       | 0.47       | 0.00       |
| MgO          | 12.87      | 13.51      | 9.32       | 1.91       | 16.38      | 9.51      | 0.34      | 0.00      | 12.12     | 9.16      | 11.25     | 18.79      | 14.68      | 19.09      | 13.34      | 21.70      |
| CaO          | 1.79       | 2.51       | 1.00       | 51.44      | 1.99       | 33.14     | 57.76     | 59.44     | 0.88      | 34.09     | 0.60      | 2.70       | 2.98       | 1.60       | 31.06      | 2.21       |
| Total        | 52.62      | 53.37      | 54.64      | 60.24      | 52.45      | 55.14     | 59.29     | 60.97     | 55.12     | 50.78     | 54.94     | 65.57      | 54.07      | 52.66      | 55.36      | 53.70      |

## Whole-rock chemistry

Major-, trace- and rare-earth element chemistry (Table 4) has been obtained for two representative samples of mafic dyke in order to ascertain its nature, classify it and to determine the regional tectonic setting at the time of the emplacement (Wang and Glover 1992; Pearce 1996 and references therein).

The presence of disseminated carbonate in the mafic dyke is reflected in the geochemical analysis with up to 8 wt. % CO<sub>2</sub>. The similar values for LOI and CO<sub>2</sub> indicate that carbonate accounts for most of the volatile component of the samples. The major-element chemistry (anhydrous) indicates that the mafic dyke is basaltic andesite, with enrichment in calcium (ca. 9 wt. % CaO) and sodium (ca. 3.5 wt. % Na<sub>2</sub>O). With respect to its chemical affinity (classification scheme of Irvine and Baragar (1971)), the dyke is subalkaline in the alkalis versus silica and normative Ol'-Ne'-Q' plots, falls near the tholeiitic - calc-alkaline boundary in the AFM plot, and conforms to a sodic-rich subalkaline suite in the normative An-Ab'-Or plot (Fig. 9). In other diagrams (not shown), the mafic dyke is tholeiitic in terms of its FeO/MgO ratio (Miyashiro 1974) and plots in the tholeiitic field of Irvine and Baragar's (1971) wt. % Al<sub>2</sub>O<sub>3</sub> versus normative An diagram.

Trace-element abundances are enriched compared to both MORB and primitive mantle values in extended trace element diagrams. They generally plot close to unity when normalized

to E-MORB (Fig. 10), except for some notable deviations due to relative enrichment (Cs, Ba, Pb, Sr) and minor depletion (Y, Yb, Lu). The trace elements Zr, Nb and Y, combined with TiO<sub>2</sub>, indicate that the dyke is of subalkaline basalt composition (Fig. 9a), thus confirming earlier classification based on the major elements.

Chondrite-normalized rare-earth element plots for two mafic dyke samples (Fig. 11) are light rare earth element (LREE) enriched and unfractionated, with (La/Sm)<sub>N</sub> about 1. However, the heavy rare earth elements (HREE) are relatively depleted and strongly fractionated ((La/Lu)<sub>N</sub> = 3). In addition, there are slightly negative Ce (Ce<sub>N</sub>/Ce\*) and positive Eu (Eu<sub>N</sub>/Eu\*) anomalies.

## STABLE ISOTOPES

Analyses of the sulphur isotopic composition of three sulphide mineral samples and carbon and oxygen isotopic compositions for two carbonate mineral samples have been obtained (Table 5) in order to constrain the nature and origin of the mineralizing fluid(s). The δ<sup>34</sup>S values for galena are +2.3 and -4.5‰, and -4.4‰ for sphalerite. Given that these results are for different samples, no estimation of equilibration between the sulphide phases is possible. The values are comparable to the sulphur isotope data for sulphide minerals from the Walton deposit (Fig. 12; Boyle *et al.* 1976), but contrast with data for the Gays River deposit, which are

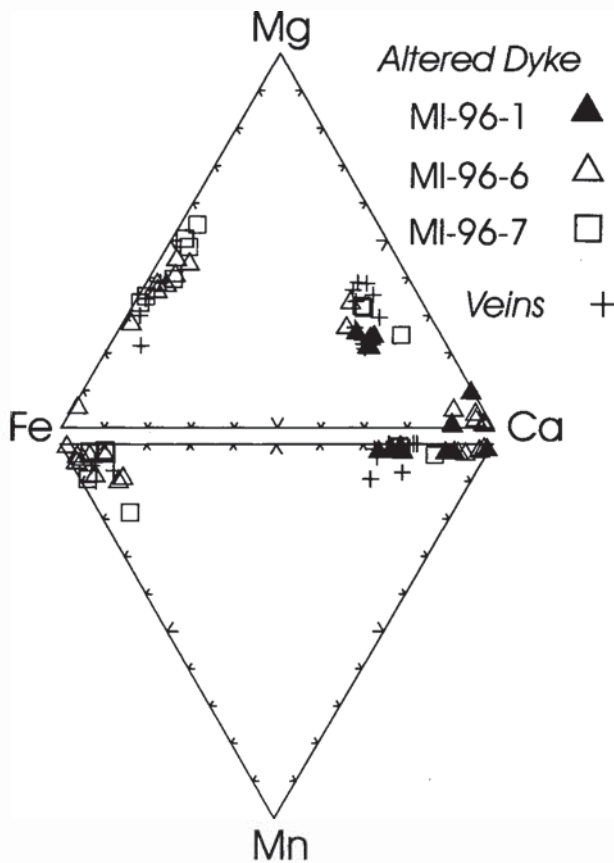


Fig. 8. Ternary plots (Fe-Ca-Mg, Fe-Ca-Mn) for carbonate phases in the matrix of three altered mafic dyke samples and veins cutting dykes and sedimentary rocks.

relatively enriched in  $^{34}\text{S}$  (Fig. 12; Akande and Zentilli 1984; Kontak 1992). Given the mineral assemblage present, it is reasonable to assume that  $\delta^{34}\text{S}_{\text{fluid}} \approx \delta^{34}\text{S}_{\text{H}_2\text{S}}$  (Ohmoto and Rye 1979); thus the  $\delta^{34}\text{S}_{\text{fluid}}$  can generally be calculated from the  $\delta^{34}\text{S}$  values of sulphide minerals if fractionation is taken into account. For example, at ca. 200°C, as determined from fluid inclusions (see below), sphalerite is enriched about 0.4‰ and galena depleted by about 2.8‰ relative to  $\text{H}_2\text{S}$  (Ohmoto and Rye 1979). Hence, the  $\delta^{34}\text{S}_{\text{fluid}}$  values are +5.1 and -1.7‰ using galena and -4.8‰ using sphalerite.

The data for two calcite samples are similar in  $\delta^{18}\text{O}$  at +22.5 and +21.2‰, but quite distinct for  $\delta^{13}\text{C}$  at -8.8 and -1.4‰, respectively. These values compare to  $\delta^{18}\text{O}$  and  $\delta^{13}\text{C}$  ranges of +12 to +20‰ and +3 to -2‰, respectively, for mineralization-stage calcite from Gays River (Akande and Zentilli 1984; Savard and Kontak 1998). Using the calcite-water fractionation equation of O'Neil *et al.* (1969),  $\delta^{18}\text{O}_{\text{water}}$  of ca. +11.7 to +13.0‰ for a temperature of ca. 200°C are calculated, but from Fig. 13 one can see that a variation of  $\pm 25^\circ\text{C}$  (i.e., formation of 175° to 225°C) does not change the  $\delta^{18}\text{O}_{\text{water}}$  substantially. The  $\delta^{13}\text{C}$  values reflect the physico-chemical conditions of the fluids at the time of carbonate formation, but given the nature of the wall rock and the sulphide assemblage, it is likely that  $\delta^{13}\text{C}_{\text{carbonate}} \approx \delta^{13}\text{C}_{\text{H}_2\text{CO}_3}$  apparent  $\approx \delta^{13}\text{C}_{\text{fluid}}$  (Ohmoto and Rye 1979); thus for the mineralizing fluids  $\delta^{13}\text{C}$  is estimated at ca. -9 to -1‰.

Table 4. Chemistry of dyke samples, Cheverie showing, Nova Scotia.

| Sample                         | MI-96-6 | MI-96-7 | MI-96-7<br>(duplicate) |
|--------------------------------|---------|---------|------------------------|
| SiO <sub>2</sub>               | 49.79   | 47.31   |                        |
| TiO <sub>2</sub>               | 1.57    | 1.37    |                        |
| Al <sub>2</sub> O <sub>3</sub> | 15.74   | 16.37   |                        |
| Fe <sub>2</sub> O <sub>3</sub> | 11.12   | 9.48    |                        |
| MnO                            | 0.19    | 0.23    |                        |
| MgO                            | 4.77    | 3.72    |                        |
| CaO                            | 7.43    | 8.57    |                        |
| Na <sub>2</sub> O              | 3.25    | 3.32    |                        |
| K <sub>2</sub> O               | 0.24    | 0.17    |                        |
| P <sub>2</sub> O <sub>5</sub>  | 0.17    | 0.15    |                        |
| L.O.I.                         | 4.93    | 7.84    |                        |
| CO <sub>2</sub>                | 5.10    | 7.99    |                        |

Trace elements (ppm; \* indicates ICP-MS)

|     |       |       |
|-----|-------|-------|
| Li* | 457.9 | 557.8 |
| Cs* | 0.61  | 0.34  |
| Ba  | 416   | 503   |
| Rb* | 7.1   | 3.5   |
| Sr* | 483   | 478.9 |
| Ga  | 18    | 19    |
| Th* | 0.81  | 0.69  |
| U*  | 0.22  | 0.17  |
| Y*  | 14.2  | 13.3  |
| Sn  | 1     | 0     |
| Sc  | 5     | 3     |
| V   | 185   | 164   |
| Cr  | 164   | 243   |
| Co  | 39    | 35    |
| Ni  | 126   | 143   |
| Cu  | 121   | 105   |
| Zn  | 104   | 64    |
| Pb* | 8.7   | 8     |
| Tl* | 0.04  | 0.05  |
| Hf* | 2.40  | 2.16  |
| Zr* | 68.44 | 62.76 |
| Nb* | 7.1   | 6.1   |
| Ta* | 0.53  | 0.35  |

Rare-earth elements (ppm; ICP-MS):

|    |       |       |       |
|----|-------|-------|-------|
| La | 5.59  | 5.13  | 5.07  |
| Ce | 13.43 | 12.27 | 12.17 |
| Pr | 2.27  | 2.05  | 2.04  |
| Nd | 11.66 | 10.28 | 10.12 |
| Sm | 3.63  | 3.20  | 3.09  |
| Eu | 1.34  | 1.21  | 1.20  |
| Gd | 3.73  | 3.58  | 3.40  |
| Tb | 0.56  | 0.51  | 0.51  |
| Dy | 3.06  | 2.90  | 2.83  |
| Ho | 0.55  | 0.56  | 0.54  |
| Er | 1.49  | 1.44  | 1.41  |
| Tm | 0.20  | 0.22  | 0.21  |
| Yb | 1.17  | 1.21  | 1.20  |

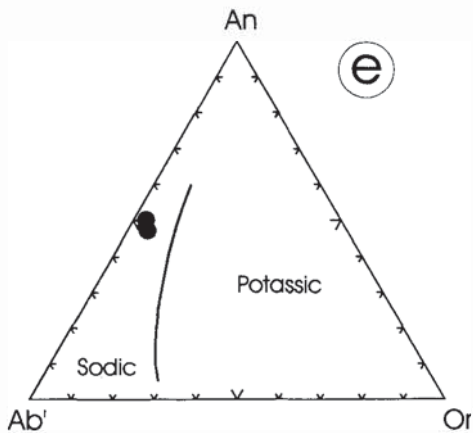
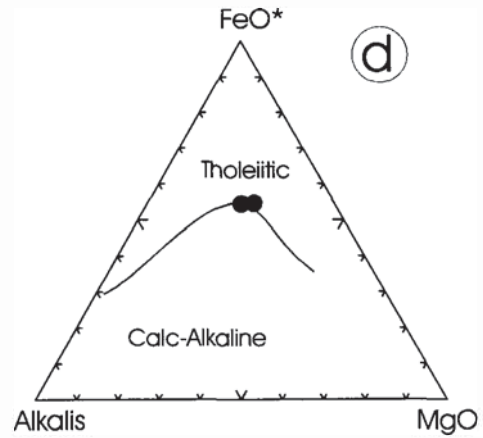
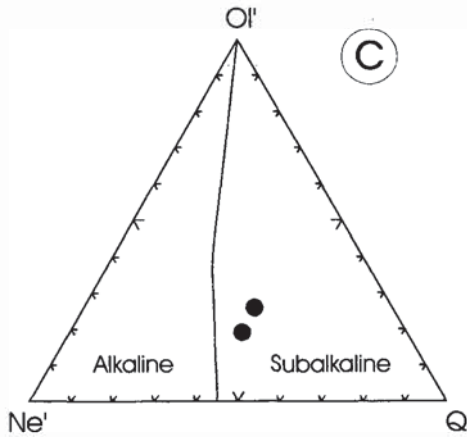
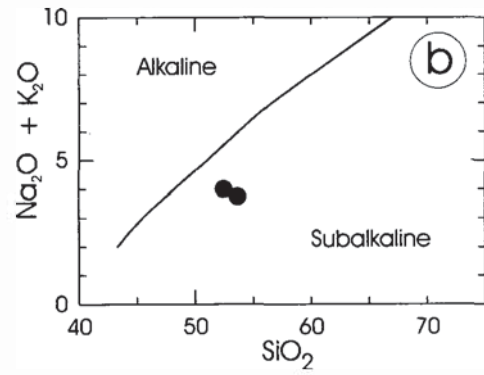
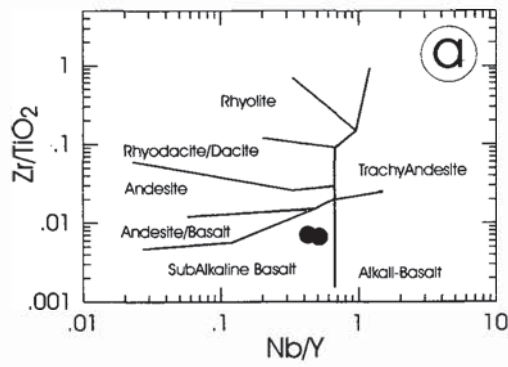


Fig. 9. Classification diagrams for mafic dyke with the data plotted as anhydrous compositions. (a)  $Zr/TiO_2$  versus  $Nb/Y$  plot (Winchester and Floyd 1977) showing the subalkaline nature of the samples and basaltic composition. (b) Alkalis versus  $SiO_2$  plot of Irvine and Baragar (1971) showing the subalkaline nature of the samples. (c) Normative  $Q'-Ne'-Ol'$  ternary plot showing the subalkaline nature of the samples (Irvine and Baragar 1971). (d) Ternary AFM plot showing the tholeiitic nature of the mafic dyke (dividing line from Irvine and Baragar 1971). (e) Ternary plot of normative  $An-Ab'-Or$  showing the sodic nature of the mafic dyke (Irvine and Baragar 1971).

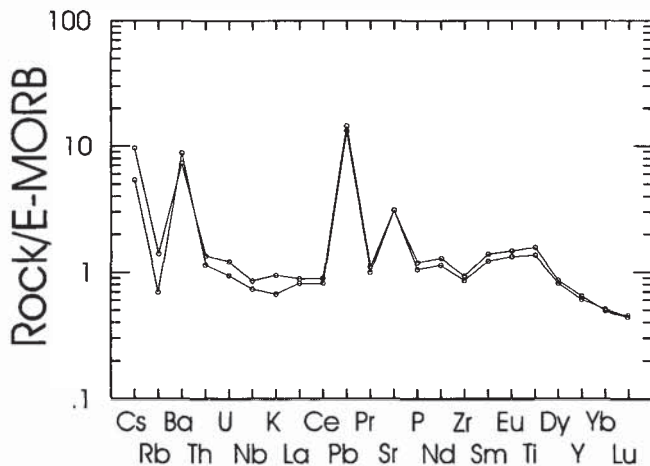


Fig. 10. Trace element or spidergram for the mafic dyke normalized to E-MORB (values of Sun and McDonough 1989).

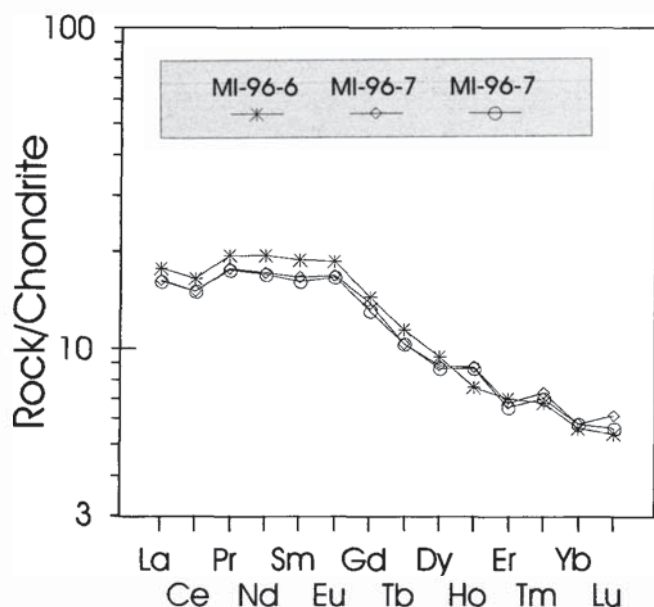


Fig. 11. Chondrite-normalized rare-earth element plot for mafic dyke. Note that for sample MI-96-7, the duplicate analysis is also shown. Chondrite normalizing factors of Taylor and McLennan (1985) were used.

## FLUID INCLUSIONS

### Petrography and classification

Various types of carbonate and quartz were examined for fluid inclusions, but only vein carbonate contained inclusions suitable for further study. The vein carbonate is generally inundated with inclusions (Fig. 14b, c), but the lack of growth zones precludes classifying the inclusions as primary. The fluid inclusions occur as two-phase liquid (L) - vapour (V) types with a large range in the L:V ratio within and between populations, which probably reflects post-entrapment modification. Monophase L- and V types also occur, with the former predominating. The monophase L- and V-rich types are considered to have formed due to necking because they do not define single fluid inclusion populations. The inclusions vary considerably in terms of size (to 75  $\mu\text{m}$ ) and shape (equant to irregular and elongate with aspect ratios of 100:1) and multiple generations of inclusions are probably present, although it was not possible to distinguish such populations based on thermometric measurements. In many cases the best inclusions are large and isolated (Fig. 14d, e, f) and characterized collectively by very uniform L:V ratios.

### Thermometric measurements

A single sample of vein carbonate hosted by altered mafic dyke and containing vein galena mineralization was used for thermometric measurements (Fig. 14a). Fluid inclusions were first frozen to  $-100^\circ\text{C}$  to  $-120^\circ\text{C}$  and slowly heated in order to determine the bulk composition of the fluid and estimate the proportion of solutes where possible (Goldstein and Reynolds 1994). Inclusions froze at temperatures of ca.  $-35^\circ\text{C}$  to  $-45^\circ\text{C}$  and  $-60^\circ\text{C}$  to  $-70^\circ\text{C}$ , with the former corresponding to higher ice melting temperatures; thus, the different freezing

Table 5. Stable isotope data for carbonate and sulphide minerals from the Cheverie showing, Nova Scotia.

| Sample  | Mineral    | $\delta^{13}\text{C}$<br>‰ | $\delta^{18}\text{O}$<br>‰ | $\delta^{34}\text{S}$<br>‰ |
|---------|------------|----------------------------|----------------------------|----------------------------|
| MI-96-1 | calcite    | -8.8                       | +22.5                      | -                          |
|         | galena     | -                          | -                          | +2.3                       |
| MI-96-4 | calcite    | -1.4                       | +21.2                      | -                          |
|         | sphalerite | -                          | -                          | -4.4                       |
| MI-96-5 | galena     | -                          | -                          | -4.5                       |

behaviours reflect different bulk compositions of the fluid inclusions (Fig. 15a). The frozen inclusions did not show signs of first melting until  $-30^\circ\text{C}$  to  $-28^\circ\text{C}$  and for most inclusions it was closer to  $-21^\circ\text{C}$ . Hydrohalite, where observed, melted at  $-23^\circ\text{C}$  to  $-21^\circ\text{C}$ . For the lowest salinity inclusions (see below), first melting occurred close to  $-3^\circ\text{C}$  to  $-1^\circ\text{C}$  with very rapid melting of ice. Last melting of ice ranged from  $-18.9^\circ\text{C}$  to  $0^\circ\text{C}$ , corresponding to salinities of 21.6 to 0 wt. % equiv. NaCl (Fig. 15b). The low-salinity nature of many of the inclusions is also reflected in the abundance of evacuated inclusions lacking decrepitate mounds, as observed during imaging on the electron microprobe (Fig. 15d). The apparent gap at 6–10 wt. % equiv. NaCl may be real or, alternatively, an artifact of sampling given the moderate amount of data. The behaviour of the inclusions during freezing runs contrasts markedly with that observed in fluid inclusion studies of basal Windsor Group-hosted mineralization in which low first-melting temperatures of ca.  $-60^\circ\text{C}$  to  $-70^\circ\text{C}$  were generally observed for the mineralizing fluids (Chi *et al.* 1995; Chi and Savard 1996; Kontak 1998; Kontak and Sangster 1998).

There were no indications (e.g., clathrate formation) from the freezing runs that condensed gases, such as  $\text{CO}_2$  or  $\text{CH}_4$ , are present in the inclusions. These gases have been reported from the Gays River and Walton deposits (Kontak 1998; Kontak and Sangster 1998).

Fluid inclusions homogenized over a range of temperatures of  $156^\circ\text{C}$  to  $265^\circ\text{C}$  (Fig. 15c), but the range within a population is much smaller ( $\leq 20$ – $30^\circ\text{C}$ ). The overall range in homogenization temperatures compares favourably with homogenization temperatures reported for basal Windsor Group mineralization (Chi *et al.* 1995; Chi and Savard 1996; Kontak 1998; Kontak and Sangster 1998).

### Decrepitate analysis

Analysis of decrepitate mounds (Haynes and Kesler 1987; Savard and Chi 1998) provide semi-quantitative data for the solute composition of inclusions. After decrepitation of fluid inclusions on the heating stage, the decrepitate mounds were imaged and analysed using the electron microprobe to determine bulk compositions. A sample of comb quartz intergrown with carbonate (Fig. 4e) was used for the decrepitate analysis. Fluid in the analysed sample is dominated by NaCl and  $\text{CaCl}_2$ , with only trace amounts of KCl, and Fe; Mg and Mn were below the detection limits of ca. 0.2 wt. %. The data are compared to decrepitate analyses for the Gays

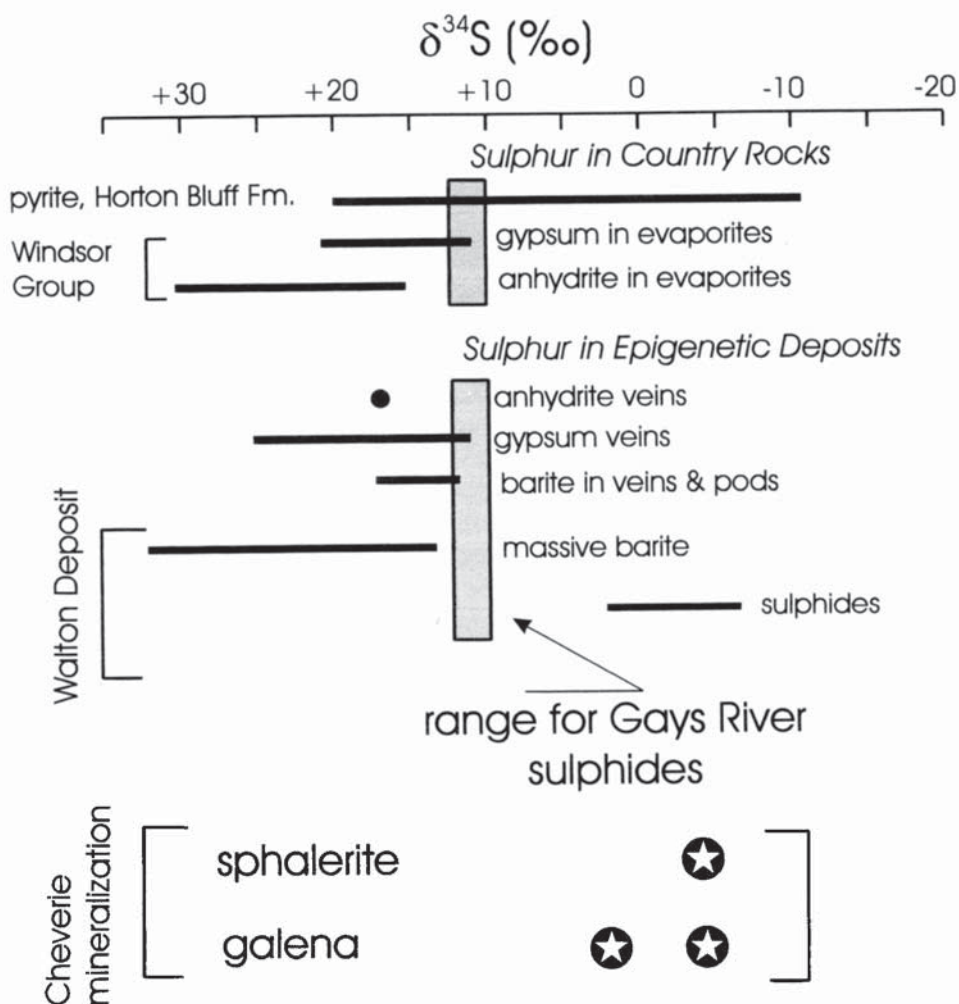


Fig. 12. Sulphur isotope data ( $\delta^{34}\text{S}$ ) for Zn-Pb sulphide mineralization at Cheverie compared to sulphur isotope data for Gays River (grey boxes) and Walton deposits (diagram modified after Kontak and Sangster (1998) using data of Boyle *et al.* (1976), Kontak (1992) and Akande and Zentilli (1984)). Note the similarity of the  $\delta^{34}\text{S}$  data for sulphides from Walton and the Cheverie showing.

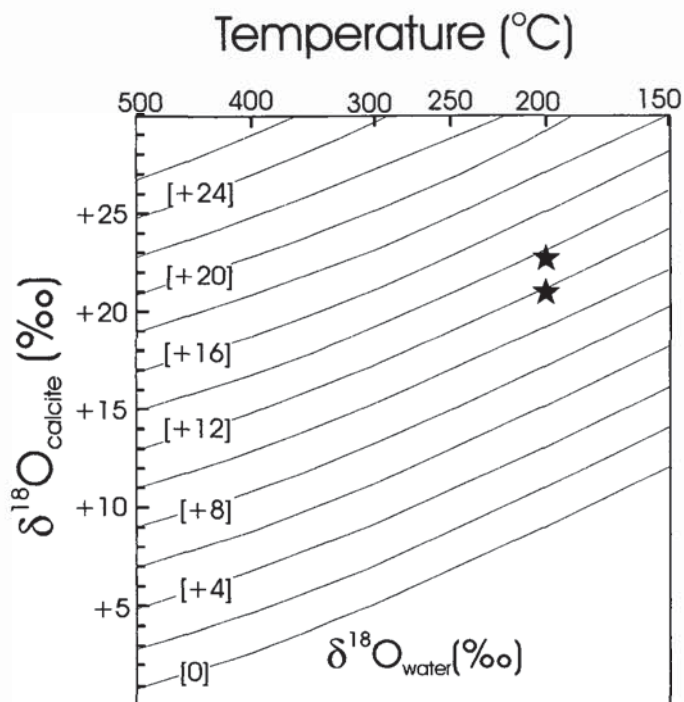


Fig. 13. Plot of  $\delta^{18}\text{O}_{\text{calcite}}$  versus temperature (°C) with isopleths (in ‰ values) for water composition ( $\delta^{18}\text{O}_{\text{water}}$ ) calculated using the fractionation equation of O'Neil *et al.* (1969). See text for discussion of the temperatures used for carbonate formation.

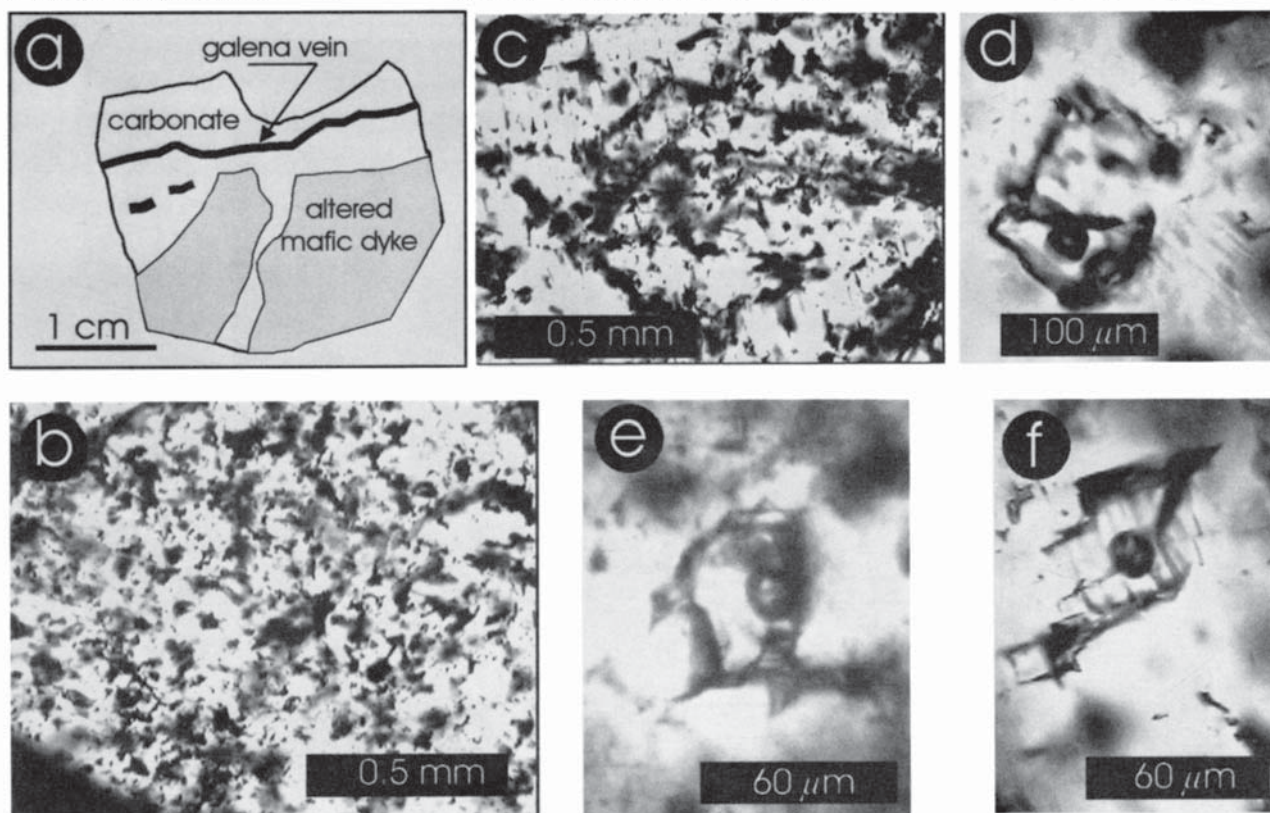


Fig. 14. Photomicrographs of fluid inclusions in vein carbonate, Cheverie showing; all photos taken in plane-polarized light. (a) Sketch of the sample used for the fluid inclusion study. (b, c) Vein carbonate with such an abundance of fluid inclusions that it is not possible to determine their origin (i.e., primary). (d, e, f). Examples of large, isolated L-V fluid inclusions. Note the similar L:V ratios for the fluid inclusions.

River and Jubilee deposits from Savard and Chi (1998) in Fig. 15e where it appears that the Cheverie fluids are, in general, slightly more Ca-rich relative to both of these other deposits.

## DISCUSSION

### Age significance of the mafic dyke

The preferred age of 315 Ma for the dyke rock corresponds to the Namurian-Westphalian time boundary (Hess and Lippolt 1986). Within the Maritimes Basin, this time is significant in that it records a period of moderately extensive deformation along parts of the Cobequid-Chedabucto Fault System and uplift of the Cobequid Highlands and related erosion of highlands and deposition of Carboniferous sediments (Calder 1998). Geological events of similar age to dyke emplacement include: (1) Alleghanian tectono-thermal activity in southwestern Nova Scotia (Kontak and Cormier 1991; Keppie and Dallmeyer 1996; Culshaw and Reynolds 1997); (2) vein-barite mineralization at  $\leq 320$  Ma in the Kinsac pluton (Kontak *et al.* 1999); (3) a thermal overprinting event in the West Gore Au-Sb deposit (Kontak *et al.* 1996); and (4) the ca. 300 Ma age for mineralization at Gays River (Pan *et al.* 1993; Kontak *et al.* 1994) and a similarly inferred age for other basal Windsor Group hosted mineralization (Ravenhurst *et al.* 1989). As summarized in Kontak *et al.* (1994), Namurian-Westphalian mafic magmatism occurs at several places in the Maritimes of eastern Canada. The Cheverie dyke provides additional

evidence for the extent of this activity. Thus, the emplacement of the mafic dyke, and perhaps of other mafic dykes in the Kennetcook Basin, may relate to regional tectonic events in the Maritimes Basin.

The implication of the ca. 315 Ma mafic dyke in terms of Carboniferous metallogeny relates to the fact that the presence of mafic magmatism may account for the local presence of elevated geothermal gradients coincident with areas of mineralization in the Carboniferous basins of the mainland, as inferred from a variety of thermal indices (e.g., fluid inclusions, clay mineralogy, organic petrography: Héroux *et al.* 1994; Kontak 1998; Kontak and Sangster 1998; Sangster *et al.* 1998a, b; Kontak *et al.* 1999).

The low-temperature overprinting age at ca.  $160 \pm 20$  Ma for sample MI-96-6 is cautiously interpreted to reflect a later thermal overprinting event. This age is obviously too young to equate to the outpouring of basaltic magma which formed the ca. 201 Ma North Mountain Basalt (Hodych and Dunning 1992) and, instead, may relate to a later thermal event.

### Source and tectonic setting of the dyke rock

Trace elements are commonly used to infer paleo-tectonic settings of basaltic rocks. Using the Ti-Zr-Y plot (Pearce 1996; Fig. 16a), a within-plate setting is indicated, which concurs with many other plots not shown (e.g., Zr/Y versus Zr, Th/Yb versus Ta/Yb, V versus Ti/1000). An anorogenic setting with transitional alkalic-tholeiitic character is suggested from the clinopyroxene chemistry (Letierrier *et al.* 1982; Fig. 16b, c). In addition to tectonic setting, the Ti-Zr-Y

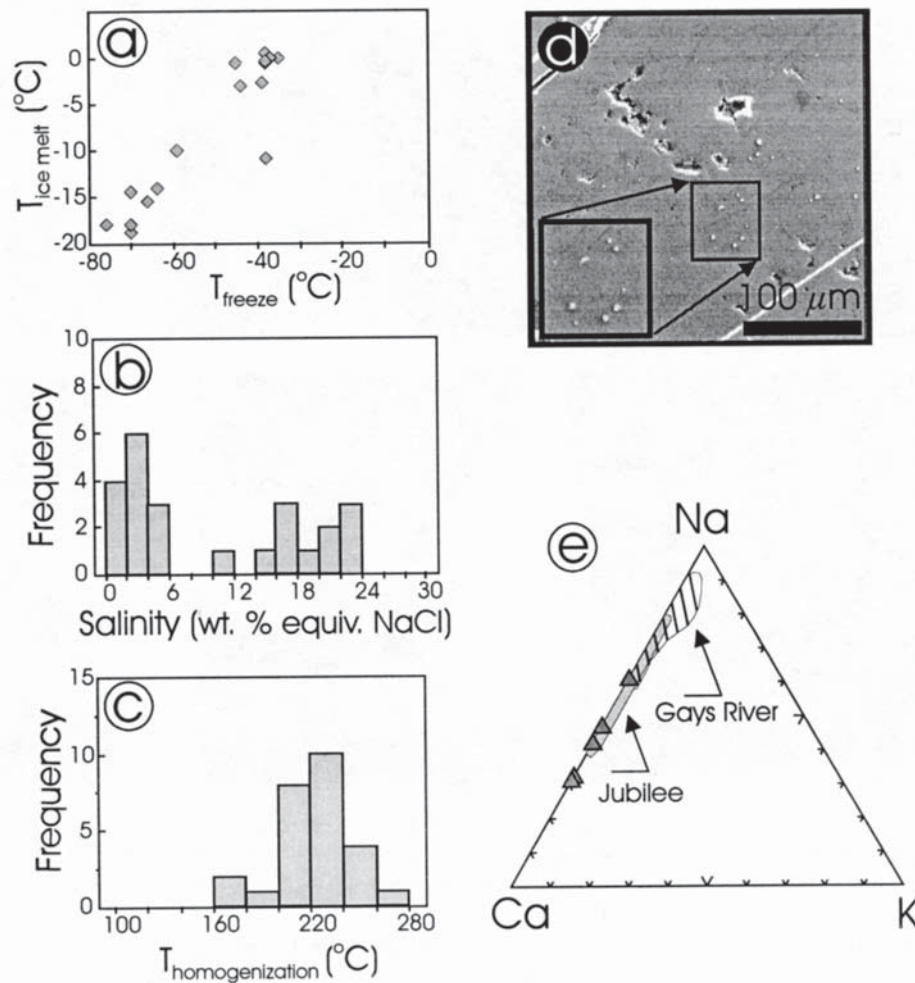


Fig. 15. Thermometric and decrepitate data for fluid inclusions from the Cheverie showing. (a) Plot of last melting temperature of ice versus freezing temperature of the inclusion. Note the strong positive correlation of the data. (b) Histogram for salinities (in wt. % equivalent NaCl) for the fluid inclusions. (c) Histogram plot of homogenization temperatures for fluid inclusions. (d) Back scattered electron (BSE) image of decrepitated fluid inclusions showing salt precipitates (i.e., small mounds in the middle of the image enlarged in the inset box) and evacuated inclusions (upper left of image). (e) Ternary Ca-Na-K plot (cation proportions) showing the Ca- and Na-rich nature of the decrepitate mounds with the compositional fields for the ore-forming fluids for the Jubilee and Gays River deposits from Savard and Chi (1998).

plot has also been used to infer petrogenesis; in this case a low percent partial melting of enriched mantle, probably garnet lherzolite, is suggested (Pearce 1996). The extended spidergram plot in Fig. 10, indicating similarity of trace elements with E-MORB, and the chondrite-normalized plot showing LREE enrichment (Fig. 11), are consistent with such a source region. The elevated contents of LILE and LREE in the extended trace element plots, falling well above MORB values, may indicate involvement of a mantle plume or hot spot (Pearce 1996). In concordance with this interpretation are the additional pertinent observations: (1) the elevated Ti/Y ratio suggests garnet as a residual phase in the source area, which implies derivation of the melt from a depth exceeding ca. 70 to 80 km (Pearce and Parkinson 1993), and (2) the lack of a significant negative Nb anomaly, the presence of which signifies an arc component, precludes a contribution from a source involved in a prior history of subduction or arc development (Pearce 1996).

The foregoing strongly suggests a deep-seated source for the mafic dyke magma, probably from an area that had

undergone some prior elemental enrichment. Initiation of melt from this source must have been in response to a larger-scale process, perhaps reflecting the broad-scale development of the Maritimes Basin, which is essentially a zone of crustal extension or lithospheric thinning. Thus, we tentatively conclude that the mafic dyke reflects tapping of a small melt fraction derived from depth. The presence of small melt fractions of magma in the form of dykes and basalt flows of Early Carboniferous age throughout the Maritimes Basin, as discussed by Kontak *et al.* (1994), may indicate periodic melting of the same source area due to a thermal anomaly. In this respect, it is relevant to note the recent suggestion of Murphy *et al.* (1999) and Keppie and Krogh (1999) that the Devonian-Carboniferous magmatic and tectonic history of the Maritime Appalachians (i.e., 400–330 Ma) may relate to the over-riding of a mantle plume. If this is correct, the presence of mafic magmatism discussed herein may relate to the prolonged effects of this event.



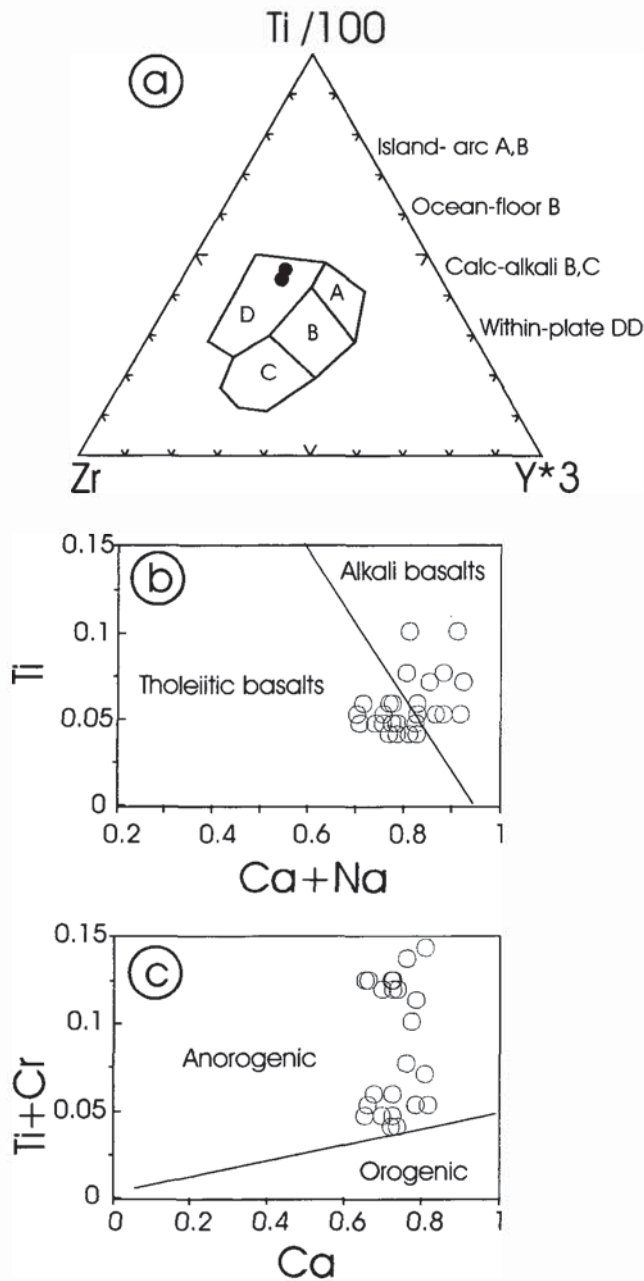


Fig. 16. Tectonic discrimination diagrams for mafic dyke samples from Cheverie. (a) Whole rock data in the Ti-Zr-Sr plot of Pearce (1996). (b, c) Clinopyroxene compositions in the discriminant diagrams of Leterrier *et al.* (1982). Note that the pyroxene data indicate a transitional nature for the mafic dyke.

#### Nature and origin of the mineralizing fluids

The salient aspects of the mineralizing fluids are the temperature of entrapment (ca. 200°C), fluid salinity (range from 0 to 24 wt. % equiv. NaCl), fluid chemistry (Na-Ca nature), and isotopic composition in terms of  $\delta^{34}\text{S}$ ,  $\delta^{18}\text{O}$ , and  $\delta^{13}\text{C}$ . These data are comparable to those documented for other areas of mineralization in the Carboniferous basins of mainland Nova Scotia (Sangster *et al.* 1998b).

In terms of the isotopic data, the nearby Walton barite, base- and precious-metal deposit formed in the presence of liquid petroleum. Conditions of the mineralizing fluids at Gays

River were somewhat similar, but mineralization did not occur in the presence of liquid petroleum; hence the difference in terms of the  $\delta^{34}\text{S}$  values of sulphide minerals (Kontak and Sangster 1998; Fig. 12). The  $\delta^{34}\text{S}$  data for Cheverie can be interpreted in two ways: (1) precipitation in the presence of liquid petroleum favours enrichment of the sulphide minerals in  $^{32}\text{S}$ ; hence low  $\delta^{34}\text{S}$  values, as recorded at Cheverie and also Walton. In this case the origin of the sulphur may have been the Windsor Group evaporites, which have  $\delta^{34}\text{S}$  of ca. +15‰; or (2) sulphide precipitation from a fluid that previously dissolved sulphide minerals with an inherently low  $\delta^{34}\text{S}$  value. The pyrite in the Horton Bluff Formation has a large range in  $\delta^{34}\text{S}$  (Boyle *et al.* 1976; see Fig. 12) and it is possible that dissolution of pyrite with the appropriate  $\delta^{34}\text{S}$  values might have occurred.

The inferred  $\delta^{18}\text{O}$  value of the fluid of ca. +13‰ compares to values of +6 to +10‰ for the main-stage mineralizing fluid at Gays River (Ravenhurst *et al.* 1987; Savard and Kontak 1998; see Fig. 13). The  $\delta^{18}\text{O}_{\text{fluid}}$  value is consistent with a fluid that has equilibrated at high temperatures with clastic sediments, in this setting perhaps the Horton Group, such as occurs for basinal fluids. However, the value is not consistent with a high-temperature fluid that exchanged with Windsor Group carbonate rocks ( $\delta^{18}\text{O}$  values of ca. +25 ‰), unless such a relatively  $^{18}\text{O}$ -rich fluid mixed with a fluid depleted in  $^{18}\text{O}$ . Alternatively, the  $\delta^{18}\text{O}_{\text{fluid}}$  value is also consistent with a local circulation model wherein local connate water convected as a result of interaction with the heated dyke rock.

The  $\delta^{13}\text{C}$  data for the carbonate samples (i.e.,  $\delta^{13}\text{C}_{\Sigma\text{C}_{\text{fluid}}} = -9$  to  $-1\%$ ) suggests a source of light carbon, which is generally indicative of bacterial processes. The organic-rich nature of the Horton Bluff Formation would be consistent with C originating in this reservoir. Given that C from petroleum has a much more depleted signature (Ohmoto and Rye 1979), it is unlikely that it owes its origin to liquid petroleum alone. The relatively heavy component of the carbon is consistent with a source in the Windsor Group such as carbonate rocks of the Macumber Formation (Savard 1996). Alternatively, the Horton Group may have provided the heavy C, but the lack of isotopic data for these rocks precludes a definitive answer. Thus, the  $\delta^{13}\text{C}$  data indicate that at least two reservoirs are required to account for the variation in the  $^{13}\text{C}$  signature of the carbonate, although the specific reservoirs cannot be identified.

The nature of the fluid, as determined from fluid inclusion studies, indicates that heated, variably saline (i.e., 0 to 24 wt.% equiv. NaCl) brines were associated with the mineralization and alteration. The high-salinity component of the fluids is similar to that of basinal brines associated with carbonate-replacement deposits or Mississippi Valley-type mineralization (see reviews in Hanor (1996) and Leach and Sangster (1995)), although the elevated temperatures are more akin to the Irish-type deposits (Hitzman and Beatty 1996). The Ca-rich nature of these fluids probably reflects fluid-rock interaction in an aquifer containing carbonate. The presence of a low-salinity fluid component indicates involvement of another fluid, also identified at the Gays River deposit (Chi and Savard 1996; Kontak 1998). As the relative timing of fluid migration is not known, it is not possible to infer whether this

low-salinity fluid was present during or after the mineralizing event.

### Formation of the Cheverie mineralization

Sangster *et al.* (1998a, b) recently discussed the nature and origin of the metalliferous fluids responsible for the Carboniferous mineralization of Nova Scotia in the context of the three main basins investigated, namely the Kennetcook, Shubenacadie-Musquodoboit and River Denys, and concluded that the fluids were basin specific. In terms of fluid generation and circulation, several mechanisms acting alone or together may have produced the mineralization, namely: (1) fluid flow related to active uplift or topography (e.g., Garven *et al.* (1993) and references therein), (2) anomalous geothermal gradients reflecting basaltic underplating (Kontak 1995; Kontak and Sangster 1995) which would enhance fluid flow, and (3) over-pressured fluids generated during compaction (e.g., Chi and Savard 1998).

The data for the Cheverie mineralization are consistent with fluids originating within the Kennetcook Basin, although the lack of Pb isotope data precludes inferring a similar reservoir for the mineralizing fluids at Walton. The solute chemistry and isotopic data reflect interaction of a moderate-temperature fluid with clastic sediments and the C and S isotopic signatures can be accounted for by source rocks of Carboniferous age. In a similar manner, fluid interaction with Horton Group clastic sediments can account for the origin of the Pb, Zn and Cu now present as mineralization at Cheverie, given the locally elevated values of these elements in the sedimentary rocks (Boyle 1972). Given the spatial association of the mafic dyke, it is tempting to relate mineralization with intrusion of the dyke; however, there is no compelling reason to do this. Thus, whereas mineralization reflects incursion of ca. 200°C mineralizing fluids, the only constraint is that they interact with the Carboniferous sediments at some time syn- or post-emplacement of the dyke at ca. 315 Ma.

### Implications for Carboniferous tectonics and metallogeny of southern Nova Scotia

The results of the present study have several important implications for Carboniferous metallogeny and tectonics, as summarized below.

1. Generation of the mafic magma reflects a persistent thermal anomaly within the mantle beneath the Maritimes Basin. This source was periodically tapped and small fractions of melt generated.
2. The presence of a thermal anomaly may have been important in terms of advecting heat into the continental lithosphere and, thereby, enhancing fluid flow within the crust. Did such fluid flow occur and was it significant in relation to mineralization? Although the present study cannot address this question, it is posed for future workers to consider.
3.  $^{40}\text{Ar}/^{39}\text{Ar}$  age spectra for two samples of the mafic dyke are interpreted to indicate an emplacement age of ca. 315 Ma based on a plateau age for the fresher of the two samples. The low temperature gas fractions suggest the presence of a later thermal event at ca. 160 Ma.

4. The timing of mineralization at Cheverie is generally similar with that at Walton and Gays River and may, therefore, reflect the same metallogenetic event.

5. The mineralization at Cheverie is similar in some respects to the element association at Walton. In addition, the presence of liquid petroleum and the sulphur isotopic data reflect interaction of the mineralizing fluid with this medium. The temptation is to assume that a similar mineralizing event has affected the two areas, which are within ca. 10 km of each other. If this analogy is correct, it clearly has implications for further mineralization in the surrounding areas.

6. A period of penetrative, ductile deformation affected rocks in the area of mineralization prior to dyke emplacement and this was followed by a period of brittle deformation. Dating of the dyke rock constrains these events to before and after ca. 315 Ma, respectively.

### ACKNOWLEDGEMENTS

This work was funded by the Nova Scotia Department of Natural Resources and D. Kontak acknowledges NSDNR management for continued support of metallogenetic studies in Nova Scotia. Stable isotope data acquired at the University of Saskatchewan and Queen's University were financed in part by NSERC operating grants to K. Ansdell and D. Archibald. D. Kontak acknowledges J. Waldron, G. Pe-Piper, B. Boehner, B. Ryan, R. Mills and R. Moore for insightful discussions with respect to the geological setting of the study area and the Maritimes Basin in general which were pertinent to this investigation, but note that these persons are not responsible for the opinions presented herein. The large thin section used in Fig. 2 was kindly provided by J. Waldron, and R. Mills provided the map used in Fig. 1c. Comments on the paper by journal reviewers and editors contributed to improving the paper and are sincerely acknowledged. This paper is published with the permission of the Director, Nova Scotia Department of Natural Resources.

### REFERENCES

- AKANDE, S., & ZENTILLI, M. 1984. Geologic, fluid inclusion and stable isotope studies of the Gays River lead-zinc deposit, Nova Scotia, Canada. *Economic Geology*, 79, pp. 1187–1211.
- BOEHNER, R.C. 1991. Seismic interpretation, potential over thrust geology and mineral deposits in the Kennetcook Basin, Nova Scotia. *In* Mines and Minerals, Report of Activities 1990, Nova Scotia Department of Mines and Energy, Report 91-1, *Edited by* D.R. MacDonald, pp. 37–47.
- BOYLE, R.W. 1972. The geology, geochemistry and origin of the barite, manganese and lead-zinc-copper-silver deposits of the Walton-Cheverie area, Nova Scotia: Geological Survey of Canada, Bulletin 166, 181 p.
- BOYLE, R.W., WANLESS, R.K., & STEVENS, R.D. 1976. Sulfur isotopic investigation of the barite, manganese and lead-zinc-copper deposits of the Walton-Cheverie area, Nova Scotia, Canada. *Economic Geology*, 71, pp. 749–762.
- CALDER, J. 1998. The Carboniferous evolution of Nova Scotia. *In* Lyell: The Past is the Key to the Present. *Edited by* D.J. Blundell and A.C. Scott. Geological Society, London, Special Publication, 143, pp. 261–302.

- CHI, G.-X., & SAVARD, M.M. 1996. Fluid evolution and mixing in the Gays River carbonate-hosted Zn-Pb deposit and its surrounding barren areas. *Atlantic Geology*, 31, pp. 141–152.
- CHI, G.-X., & SAVARD, M.M. 1998. Basinal fluid flow models related to Zn-Pb mineralization in the southern margin of the Maritimes Basin, eastern Canada. *Economic Geology*, 93, pp. 896–910.
- CHI, G.-X., SAVARD, M., & HÉROUX, Y. 1995. Constraints from fluid-inclusion data on the origin of the Jubilee carbonate-hosted Zn-Pb deposit, Cape Breton, Nova Scotia. *Canadian Mineralogist*, 33, pp. 709–722.
- CLARK, A.H., ARCHIBALD, D.A., LEE, A.W., FARRAR, E., & HODGSON, C.J. 1998. Laser probe  $^{40}\text{Ar}/^{39}\text{Ar}$  ages of early- and late-stage alteration assemblages, Rosario porphyry copper-molybdenum deposit, Collahuasi district, I Region, Chile. *Economic Geology*, 93, pp. 326–337.
- CULSHAW, N., & REYNOLDS, P.H. 1997.  $^{40}\text{Ar}/^{39}\text{Ar}$  age of shear zones in the southwest Meguma Zone between Yarmouth and Meteghan, Nova Scotia. *Canadian Journal of Earth Sciences*, 34, pp. 848–853.
- GARVEN, G., GE, S., PERSON, M.A., & SVERJENSKY, D.A. 1993. Genesis of stratabound ore deposits in the Midcontinent Basins of North America. I. The role of regional groundwater flow. *American Journal of Science*, 293, pp. 497–568.
- GOLDSTEIN, R.H., & REYNOLDS, T.J. 1994. Systematics of fluid inclusions in diagenetic minerals. *Society for Sedimentary Geology Short Course* 31, 199 p.
- HANOR, J.S. 1996. Controls on the solubilization of lead and zinc in basinal brines. In *Carbonate-Hosted Lead-Zinc Deposits*, Edited by D.F. Sangster. Society of Economic Geologists, Special Publication No. 4, pp. 483–500.
- HAYNES, F.M., & KESLER, S.E. 1987. Chemical evolution of brines during Mississippi Valley-type mineralization: Evidence from East Tennessee and Pine Point. *Economic Geology*, 82, pp. 53–71.
- HÉROUX, Y., CHAGNON, A., & SAVARD, M.M. 1994. Anomalies des propriétés de la matière organique et des assemblages argileux associées au gîte de Pb-Zn de Gays River, Nouvelle-Écosse, Canada. *Exploration and Mining Geology*, 3, pp. 67–79.
- HESS, J.L., & LIPPOLT, H.J. 1986.  $^{40}\text{Ar}/^{39}\text{Ar}$  ages of tonstein and sandines: new calibration points for the improvement of the Upper Carboniferous time scale. *Chemical Geology (Isotope Geoscience Section)*, 59, pp. 143–154.
- HITZMAN, M.W., & BEATY, D.W. 1996. The Irish Zn-Pb-(Ba) Orefield. In *Carbonate-Hosted Lead-Zinc Deposits*, Edited by D.F. Sangster. Society of Economic Geologists, Special Publication No. 4, pp. 112–143.
- HODYCH, J.P., & DUNNING, G.R. 1992. Did the Manicouagan impact trigger end-of-Triassic mass extinction? *Geology*, 20, pp. 51–54.
- IRVINE, T.N., & BARAGAR, W.R.A. 1971. A guide to the chemical classification of the common volcanic rocks. *Canadian Journal of Earth Sciences*, 8, pp. 523–548.
- JENNER, G.A., LONGERICH, H.P., JACKSON, S.E., & FRYER, B.J. 1990. ICP-MS - a powerful tool for high precision trace element analysis in earth sciences: evidence from analysis of selected USGS reference samples. *Chemical Geology*, 83, pp. 133–148.
- JOHNSON, S.K. 1999. Structural geology of the Horton and Windsor Groups, Cheverie, Nova Scotia. Unpublished B.Sc. thesis, St. Mary's University, Halifax, Nova Scotia, 89 p.
- KEPPIE, J.D., & DALLMEYER, R.D. 1996. Late Paleozoic collision, delamination, short-lived magmatism, and rapid denudation in the Meguma Terrane (Nova Scotia, Canada): constraints  $^{40}\text{Ar}/^{39}\text{Ar}$  isotopic data. *Canadian Journal of Earth Sciences*, 32, pp. 644–659.
- KEPPIE, J.D., & KROGH, T.E. 1999. U-Pb geochronology of Devonian Granites in the Meguma Terrane of Nova Scotia, Canada: Evidence for hot spot melting of a Neoproterozoic source. *Journal of Geology*, 107, pp. 555–568.
- KONTAK, D.J. 1992. A preliminary report on geological, geochemical, fluid inclusion and isotopic studies of the Gays River Zn-Pb deposit, Nova Scotia: Nova Scotia Department Natural Resources, Open File Report 92-014, 223 p.
- KONTAK, D.J. 1995. Geological and geochemical studies of the carbonate-hosted Gays River Zn-Pb deposit, Nova Scotia: Mineralization from high temperature, saline brines related to underplating by basaltic magma. In *International Field Conference on Carbonate-Hosted Lead Zinc Deposits: Society of Economic Geologists*. Edited by D.L. Leach and M.B. Goldhaber, Co-general Chairmen, pp. 154–158.
- KONTAK, D.J. 1998. A study of fluid inclusions in sulfide and non-sulfide phases from a carbonate-hosted Zn-Pb deposit, Nova Scotia. *Economic Geology*, 93, pp. 793–817.
- KONTAK, D.J., & CORMIER, R.F. 1991. Geochronological evidence for multiple tectono-thermal overprinting events in the East Kemptville muscovite-topaz leucogranite, Yarmouth County, Nova Scotia, Canada. *Canadian Journal of Earth Sciences*, 28, pp. 209–224.
- KONTAK, D.J., & KERRICH, R. 1997. An isotopic (C, O, Sr) study of vein quartz and carbonate from Meguma gold deposits, Nova Scotia, Canada. *Economic Geology*, 92, pp. 161–180.
- KONTAK, D.J., & SANGSTER, D.F. 1995. Fluid inclusion studies of barite from the Walton (Ba-Zn-Pb-Cu-Ag) deposit, Kennetcook Basin, Nova Scotia: nature and origin of petroleum in a carbonate-hosted replacement deposit. In *International Field Conference on Carbonate-Hosted Lead Zinc Deposits: Society of Economic Geologists*. Edited by D.L. Leach and M.B. Goldhaber, Co-general Chairmen, pp. 154–158, pp. 159–162.
- KONTAK, D.J., & SANGSTER, D.J. 1998. A fluid inclusion study of aqueous and petroleum inclusions in the Walton Na-Pb-Zn-Cu-Ag deposit, Nova Scotia. *Economic Geology*, 93, pp. 845–868.
- KONTAK, D.J., MCBRIDE, S.L., & FARRAR, E. 1994.  $^{40}\text{Ar}/^{39}\text{Ar}$  dating of fluid migration in a Mississippi-Valley type deposit: Gays River Zn-Pb deposit, Nova Scotia. *Economic Geology*, 89, pp. 1501–1517.
- KONTAK, D.J., SMITH, P.K., & HORNE, R.J. 1996. Hydrothermal characterization of the West Gore Au-Sb deposit, Meguma Terrane, Nova Scotia. *Economic Geology*, 91, pp. 1239–1262.
- KONTAK, D.J., HORNE, R.J., ANSDALL, K., & ARCHIBALD, D.A. 1999. Carboniferous barite-fluorite mineralization in the Devonian Kinsac Pluton, southern Nova Scotia. *Atlantic Geology*, 35, pp. 109–127.
- LEACH, D., & SANGSTER, D.F. 1995. Mississippi Valley-type lead-zinc deposits. *Geological Association of Canada Special Paper* 40, pp. 289–314.
- LETERRIER, J., MAURY, R.C., THONON, P., GIRARD, D., & MARCHA, M. 1982. Clinopyroxene composition as a method of identification of the magmatic affinities of paleo-volcanic series. *Earth and Planetary Science Letters*, 59, pp. 139–154.
- MACISSAC, J. 1998. Cheverie base metal project, Hants County, Nova Scotia. In *Mining Matters for Nova Scotia '98*, Edited by D.R. MacDonald, Nova Scotia Department of Natural Resources, Report 98-2, p. 20.
- MCDOUGALL, I., & HARRISON, T.M. 1988. Geochronology and thermochronology by the  $^{40}\text{Ar}/^{39}\text{Ar}$  method. *Oxford Monographs on Geology and Geophysics* No. 9, 212 p.
- MIYASHIRO, A. 1974. Volcanic rocks series in island arcs and active continental margins. *American Journal of Science*, 274, pp. 321–355.
- MOORE, R.G., FERGUSON, S.A., BOEHNER, R.C. AND KENNEDY, C.M. 2000. Wolfville/Windsor area (NTS sheets 21H/01 and part of NTS sheet 21A/16) Hants and Kings Counties. Scale 1:50 000. Nova Scotia Department of Natural Resources, Open File Map 2000-03.
- MURPHY, J.B., VAN STAAL, C., & KEPPIE, J.D. 1999. The Middle to Late Paleozoic Acadian Orogeny in the northern Appalachians:

- a Laramide-style plume-modified orogeny: *Geology*, 27, pp. 653–656.
- OHMOTO, H., & RYE, D. 1979. Isotopes of sulfur and carbon, *In* *Geochemistry of Hydrothermal Ore Deposits*. Edited by H.L. Barnes. John Wiley & Sons, New York, pp. 509–567.
- O'NEIL, J.R., CLAYTON, R.N., & MAYEDA, T.K. 1969. Oxygen isotope fractionation in divalent metal carbonates. *Journal of Chemistry and Physics*, 51, pp. 5547–5558.
- PAN, H., SYMONS, D.T.A., & SANGSTER, D.F. 1993. Paleomagnetism of the Gays River zinc-lead deposit, Nova Scotia: Pennsylvanian ore genesis. *Geophysical Research Letters*, 20, pp. 1159–1162.
- PEARCE, J.A. 1996. A users guide to basalt discrimination diagrams. *In* *Trace Element geochemistry of Volcanic Rocks: Applications for Massive Sulphide Exploration*. Edited by D.A. Wyman. Geological Association of Canada, Short Course Notes, 12, pp. 79–113.
- PEARCE, J.A., & PARKINSON, I.J. 1993. Trace element models for mantle melting: applications to volcanic arc petrogenesis. *Geological Society London, Special Publications*, 76, pp. 373–403.
- RAVENHURST, C.E., REYNOLDS, P.H., & ZENTILLI, M. 1987. Isotopic constraints on the genesis of Zn-Pb mineralization at Gays River, Nova Scotia, Canada. *Economic Geology*, 82, pp. 1294–1308.
- RAVENHURST, C.E., REYNOLDS, P. H., ZENTILLI, M., KRUEGER, H. W., & BLENKINSOP, J. 1989. Formation of Carboniferous Pb-Zn and barite mineralization from basin-derived fluids, Nova Scotia, Canada. *Economic Geology*, 84, pp. 1471–1488.
- SANGSTER, D.F., & SAVARD, M.M. 1998. Introduction: A special issue devoted to zinc-lead mineralization and basinal brine movement, Lower Windsor Group (Viséan), Nova Scotia, Canada. *Economic Geology*, 93, pp. 699–702.
- SANGSTER, D.F., SAVARD, M.M., & KONTAK, D.J. 1998a. Sub-basin specific Pb and Sr sources in Zn-Pb deposits of the Lower Windsor Group, Nova Scotia. *Economic Geology*, 93, pp. 923–931.
- SANGSTER, D.F., SAVARD, M.M., & KONTAK, D.J. 1998b. A genetic model for mineralization of Lower (Viséan) carbonate rocks of Nova Scotia, Canada. *Economic Geology*, 93, pp. 932–952.
- SAVARD, M.M. 1996. Pre-ore burial dolomitization adjacent to the carbonate-hosted Gays River Zn-Pb deposit, Nova Scotia. *Canadian Journal of Earth Sciences*, 33, pp. 303–315.
- SAVARD, M.M., & CHI, G.X. 1998. Cation study of fluid inclusion decrepitates in the Jubilee and Gays River (Canada) Zn-Pb deposits - characterization of ore-forming brines. *Economic Geology*, 93, pp. 920–931.
- SAVARD, M.M., & KONTAK, D.J. 1998.  $^{13}\text{C}$ - $^{18}\text{O}$ - $^{87}\text{Sr}/^{86}\text{Sr}$  co-variations in ore-stage calcites in and around the Gays River Zn-Pb deposit, Nova Scotia - evidence for fluid mixing. *Economic Geology*, 93, pp. 818–833.
- STEVENSON, I.M. 1959. Shubenacadie and Kennetcook map-areas, Colchester, Hants and Halifax counties, Nova Scotia. *Geological Survey of Canada, Memoir* 302, 88 p.
- SUN, S.S., & MCDONOUGH, W.F. 1989. Chemical and isotopic systematics of ocean basalts: implications for mantle composition and processes. *In* *Magmatism in the Ocean Basins*. Edited by A.D. Saunders and M.J. Norry. Geological Society London, Special Publications, vol. 42, pp. 313–345.
- TAYLOR, S.R. & MCLENNAN, S.M. 1985. *The Continental Crust: its Composition and Evolution*. Blackwell Scientific.
- TURNER, G. 1968. The distribution of potassium and argon in chondrites. *In* *Origin and Distribution of the Elements*. Edited by L.H. Ahrens, Pergamon, London, pp. 387–398.
- WANG, P., & GLOVER, L. 1992. A tectonics test of the most commonly used geochemical discriminant diagrams and patterns. *Earth Science Reviews*, 33, pp. 111–131.
- WINCHESTER, J.A., & FLOYD, P.A. 1977. Geochemical discrimination of different magma series and their differentiation products using immobile elements. *Chemical Geology*, 20, pp. 325–343.

Editorial responsibility: Sandra M. Barr